ANNUAL REVIEWS

Annual Review of Physical Chemistry

Triplet-Pair States in Organic Semiconductors

Andrew J. Musser and Jenny Clark

Department of Physics and Astronomy, University of Sheffield, Sheffield S3 7RH, United Kingdom; email: a.musser@sheffield.ac.uk, jenny.clark@sheffield.ac.uk

Annu. Rev. Phys. Chem. 2019. 70:323–51

The *Annual Review of Physical Chemistry* is online at physchem.annualreviews.org

https://doi.org/10.1146/annurev-physchem-042018-052435

Keywords

triplet pair, entanglement, quintet, singlet fission, triplet-triplet annihilation, exchange coupling

Abstract

Entanglement of states is one of the most surprising and counterintuitive consequences of quantum mechanics, with potent applications in cryptography and computing. In organic semiconductor materials, one particularly significant manifestation is the spin-entangled triplet-pair state, which consists of a pair of localized triplet excitons coupled into an overall spin-0, -1, or -2 configuration. The most widely analyzed of these is the spin-0 pair, denoted ^{1}(TT), which was initially invoked in the 1960s to explain delayed fluorescence in acene films. It is considered an essential gateway state for triplet-triplet annihilation and the reverse process, singlet fission, enabling interconversion between one singlet and two triplet excitons without any change in overall spin. This state has returned to the forefront of organic materials research in recent years, thanks both to its central role in the resurgent field of singlet fission and to its implication in a host of exotic new photophysical behaviors. Here we review the properties of triplet-pair states, from first principles to recent experimental results.

1. INTRODUCTION

In its simplest description, a triplet-pair state is made up of two correlated triplet (spin $S = 1$) states. In the field of organic optoelectronics, these triplet-pair states have received a lot of interest in recent years because of their role in singlet exciton fission, where a pair of triplets is created from a single absorbed photon. This two-for-one process has the potential to be harnessed in solar cells to beat the Shockley–Queisser limit, offering the opportunity of increasing power conversion efficiency of even the most efficient solar cells (1). Additional interest in triplet-pair states stems from the fact that the triplets within the pair are spin-entangled and could remain so even as they separate (2).

Triplet pairs can also be formed from the encounter of two triplets, for example, in upconversion materials, resulting in an encounter complex triplet pair that, with the correct spin configuration, can fuse to form a singlet exciton that emits. In both singlet fission and triplet fusion, the triplet-pair state is an elusive state whose electronic and spin properties remain an area of active research.

Triplet pairs are generally dark (nonemissive) and therefore often require indirect or multiple experimental probes to uncover their nature and behavior. At the same time, theoretical descriptions of multiexciton states in large and multimolecule systems push the boundaries of available theoretical techniques (3). Our understanding of triplet-pair states in organic semiconductors has progressed very rapidly over the past few years, and here we review this progress and describe our current understanding. This review deals specifically with the nature and behavior of triplet-pair states, rather than the processes of singlet fission or triplet fusion (triplet-triplet annihilation), which have been reviewed elsewhere (1, 3–13).

2. BACKGROUND

A useful starting point when describing the triplet-pair states (see, e.g., 14) is their constituent triplets. We therefore begin by describing two-electron states.

2.1. Two-Electron Singlet and Triplet States

In an isolated closed-shell molecule in which the electrons have paired spins in the ground state, promoting an electron from the highest occupied molecular orbital (HOMO) to the lowest unoccupied molecular orbital (LUMO) results in a two-electron excited state, often described as an exciton (15, 16). This state can be described by a spatial wave function Φ and a spin wave function χ, where the overall wave function is $\Psi = \Phi\chi$. In terms of spin, the two unpaired electrons have four possible combinations: $|\alpha\alpha\rangle$, $|\alpha\beta\rangle$, $|\beta\alpha\rangle$, and $|\beta\beta\rangle$ (see **Figure 1**), where $|\alpha\rangle$ and $|\beta\rangle$ are the usual eigenstates of the one-electron spin operators $\hat{\mathbf{S}}_1^2$ and $\hat{S}_{1z}$. These four combinations are not eigenstates of the two-electron spin Hamiltonian, which are found by diagonalizing the matrix of the total spin angular momentum operator: $\hat{\mathbf{S}}^2 = \left(\hat{\mathbf{S}}_1 + \hat{\mathbf{S}}_2\right)^2$. Diagonalizing $\hat{\mathbf{S}}^2$ results in four pure spin states: one singlet ($S = 0$) and three triplets ($S = 1$) (14, 17):

$$
\begin{aligned}
|S_1^{(2)}\rangle &= \frac{1}{\sqrt{2}}\left(|\alpha_1\beta_2\rangle - |\beta_1\alpha_2\rangle\right),\\
|T_{-1}^{(2)}\rangle &= |-\rangle = |\beta_1\beta_2\rangle\\
|T_0^{(2)}\rangle &= |0\rangle = \frac{1}{\sqrt{2}}\left(|\alpha_1\beta_2\rangle + |\beta_1\alpha_2\rangle\right),\\
|T_{+1}^{(2)}\rangle &= |+\rangle = |\alpha_1\alpha_2\rangle.
\end{aligned}
\qquad 1.
$$

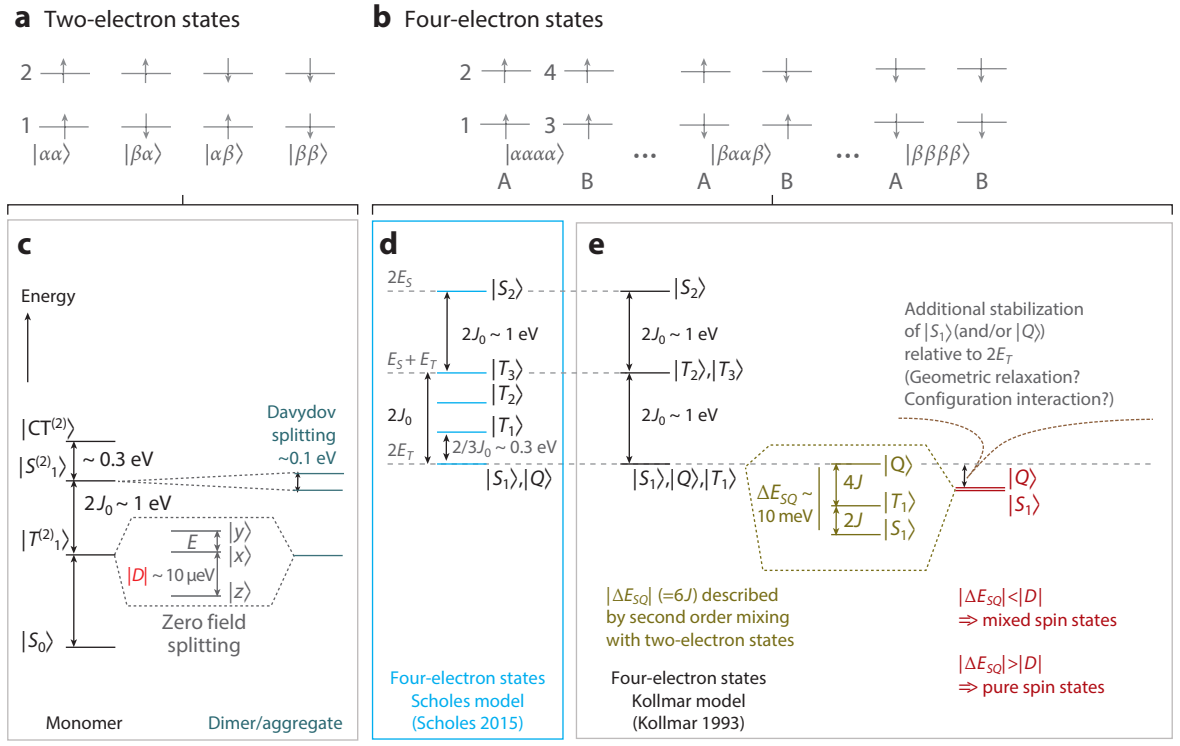

Figure 1

The (*a*) two-electron and (*b*) four-electron product basis states, where $|\alpha\rangle$ and $|\beta\rangle$ are the usual spin-up and spin-down single-electron states. (*c*) The relative energies of the two-electron states (with two-electron states denoted by a superscript 2, omitted for the four-electron states), including the fine structure of the triplets $|x\rangle$, $|y\rangle$, and $|z\rangle$ (Equation 3) given by the zero-field-splitting E and D parameters (Equation 4). In singlet-fission materials, D is $\sim 10^5$ times smaller than half the singlet/triplet splitting J_0 [i.e., exchange energy J_0, defined as half the energetic separation between $|S_1^{(2)}\rangle$ and $|T_1^{(2)}\rangle$]. The Davydov splitting in aggregates/crystals due to resonant energy transfer and mixing between Frenkel excitons and charge-transfer excitons is shown for comparison (15, 16, 136). (*d*) The relative energies of the four-electron states according to Scholes (2), who suggested that $|S_1\rangle$ (i.e., the spin-0 triplet pair) is not degenerate with any four-electron $S = 1$ triplet state, $|T_1\rangle$. (*e*) The relative energies of the four-electron states according to Kollmar (22), who, in contrast, suggested that $|S_1\rangle$, $|Q\rangle$, and $|T_1\rangle$ are all triplet-pair states and degenerate at two times the triplet energy E_T. Also shown is the fine-structure splitting of the lowest-lying $|S_1\rangle$, $|Q\rangle$, and $|T_1\rangle$ states due to the exchange term J in Equation 6, which can be described by a configuration interaction that mixes the four-electron states with two-electron charge-transfer or exciton states. ΔE_{SQ} is often taken to be the binding energy of $|S_1\rangle = {}^1(\mathrm{TT})$ (40). $\Delta E_{SQ} \approx 6J$ is estimated to be on the order of 10 meV (28, 31, 65). Stabilization of $|S_1\rangle$ and/or $|Q\rangle$ with respect to $2E_T$ may be on the order of 100 meV (e.g., in tetracene-like materials). The origin of this stabilization is not yet established.

Here $|\alpha_i\rangle$ and $|\beta_i\rangle$ are the usual single-electron spin functions, where the indices refer to electron 1 or 2; the superscript on $|S\rangle$ or $|T\rangle$ refers to the number of electron spins and the subscript to the M_s quantum number. As $|T_n^{(2)}\rangle$ are eigenstates of both $\hat{\mathbf{S}}^2$ and $\hat{S}_z$, they are often referred to as the high-field basis since they describe the eigenstates when a magnetic field B_z is applied to the system. In the literature, these eigenstates are also defined as the $|-\rangle$, $|0\rangle$, and $|+\rangle$ states, using the M_s eigenvalue notation.

The three triplet states are symmetric when exchanging an electron from orbital 1 to orbital 2 (HOMO to LUMO). Therefore, the spatial component of the wave function must be antisymmetric according to the Pauli exclusion principle. Likewise, the singlet has an antisymmetric spin wave function but a symmetric spatial wave function. As the spatial part of the triplet wave

functions must contain a node, the Coulomb repulsion is lower. As a result, the triplet energy is lower than that of the singlet by an amount proportional to the exchange energy $2J_0$, defined as the energetic separation between $|S_1^{(2)}\rangle$ and $|T_1^{(2)}\rangle$ (see **Figure 1*c***). In π-conjugated molecules, $2J_0$ is on the order of ~0.5–1 eV.

In the absence of a magnetic field, the spins of the two electrons can interact, via a spin dipole-dipole or spin-orbit interaction. The spin-orbit interaction is usually neglected in π-conjugated hydrocarbons, although this may depend on nonadiabatic coupling (18). Neglecting spin-orbit interaction, the dipolar interaction leads to splitting of the three triplets into sublevels. The zero-field-splitting Hamiltonian is given by

$$\hat{H}_{\mathrm{ZFS}} = \hat{\mathbf{S}} \cdot \mathbf{D} \cdot \hat{\mathbf{S}}, \qquad 2.$$

where **D** is a symmetric, traceless tensor that contains details of the spin-spin interaction. It can be diagonalized by choosing a suitable coordinate system, termed principal axes: x, y, and z. The principal axes are arbitrary and are usually defined so that the z direction has the largest dipolar coupling strength. With the molecular coordinate system, the three triplet states become

$$\begin{aligned} |x\rangle &= \frac{1}{\sqrt{2}}\left(|\beta\beta\rangle - |\alpha\alpha\rangle\right), \\ |y\rangle &= \frac{i}{\sqrt{2}}\left(|\beta\beta\rangle + |\alpha\alpha\rangle\right), \\ |z\rangle &= \frac{1}{\sqrt{2}}\left(|\alpha\beta\rangle + |\beta\alpha\rangle\right). \end{aligned} \qquad 3.$$

Note that either of the triplet basis sets in Equation 1 or 3 can be used to provide a complete description of the two-electron triplet subspace. The basis set chosen depends on the experimental observable. The relative energies of the three states in Equation 3 can be defined by the so-called D and E parameters (14, 19) (see **Figure 1**). These values are usually small in π-conjugated molecules, typically $\sim 10^{-5} J_0 \sim 10$ μeV. Defining X, Y, and Z as the relative energies of $|x\rangle$, $|y\rangle$, and $|z\rangle$ (such that $\hat{H}_{\mathrm{ZFS}}|x\rangle = X|x\rangle$, etc.), one obtains $D = \frac{3Z}{2}$ and $E = \frac{X-Y}{2}$. By convention, D and E are defined such that $|D| \geq 3|E|$ and $|D_z| \geq |D_x| \geq |D_y|$ (20). From these definitions of D and E, the zero-field-splitting Hamiltonian can be written as

$$\begin{aligned} \hat{H}_{\mathrm{ZFS}} &= -X\hat{S}_x^2 - Y\hat{S}_y^2 - Z\hat{S}_z^2, \\ \hat{H}_{\mathrm{ZFS}} &= D\left[\hat{S}_z^2 - \frac{\hat{\mathbf{S}}^2}{3}\right] + E\left[\hat{S}_x^2 - \hat{S}_y^2\right]. \end{aligned} \qquad 4.$$

In analogy with the classical dipole-dipole interaction, and assuming point dipoles, the zero-field-splitting parameters D and E can be formulated as $D = \frac{3}{4}\frac{\mu_0}{4\pi\hbar}(g_e\mu_B)^2\langle\frac{r^2-3z^2}{r^5}\rangle = \frac{3}{4}\frac{\mu_0}{4\pi\hbar}(g_e\mu_B)^2\langle\frac{1-3\cos^2\theta}{r^3}\rangle$ and $E = \frac{3}{4}\frac{\mu_0}{4\pi\hbar}(g_e\mu_B)^2\langle\frac{y^2-x^2}{r^5}\rangle$, where r is the distance between unpaired electron spins, θ is the angle between the spin vector and the dipolar z-axis, and the angular brackets denote the expectation value (20). Therefore, provided the point-dipole approximation holds, D can be related to the average interspin distance and can be used to estimate the size of the triplet exciton (20, 21), ~1.38 Å (1.5 benzene rings) in tetracene (21). E contains information about the rhombicity of the zero-field-splitting tensor (20) and is zero in axially symmetric molecules.

2.2. Four-Electron Singlet, Triplet, and Quintet States

Having described the two-electron triplet and singlet states, their basis states, and energies (**Figure 1*a*,*c***), we move on to describe the four-electron states, which include triplet-pair states. A four-electron system is extremely complex and cannot be solved through simple diagonalization of a Hamiltonian, as done for the two-electron states above. However, in the context of this review, it is useful to describe the triplet-pair states to first order using a model Hamiltonian (2, 3, 14, 22, 23).

This model assumes four electrons on sites A and B (see **Figure 1*b***). Starting with these four electrons, we can write 16 products: $|\alpha\alpha\alpha\alpha\rangle$, $|\alpha\alpha\alpha\beta\rangle \ldots |\beta\beta\beta\beta\rangle$, where $|\alpha\rangle$ and $|\beta\rangle$ are the usual one-electron spin eigenstates described above. These product states are not eigenstates of $\hat{\mathbf{S}}^2 = (\hat{\mathbf{S}}_1 + \hat{\mathbf{S}}_2 + \hat{\mathbf{S}}_3 + \hat{\mathbf{S}}_4)^2$, but using them to diagonalize $\hat{\mathbf{S}}^2$ results in 16 pure spin states: 2 with $S = 0$ (singlet $|S_n\rangle$), 9 with $S = 1$ (triplet $|T_n\rangle$), and 5 with $S = 2$ (quintet $|Q\rangle$). Equation 5 shows the spin part of the six four-electron spin wave functions that have $M_S = 0$, according to Kollmar (22):

$$
\begin{aligned}
\text{Singlet 1} &: |S_1\rangle = \frac{1}{\sqrt{12}}(2\,|\alpha\alpha\beta\beta\rangle + 2\,|\beta\beta\alpha\alpha\rangle - |\alpha\beta\alpha\beta\rangle - |\beta\alpha\alpha\beta\rangle - |\alpha\beta\beta\alpha\rangle - |\beta\alpha\beta\alpha\rangle),\\
\text{Singlet 2} &: |S_2\rangle = \frac{1}{2}\,(|\alpha\beta\alpha\beta\rangle - |\beta\alpha\alpha\beta\rangle - |\alpha\beta\beta\alpha\rangle + |\beta\alpha\beta\alpha\rangle),\\
\text{Triplet 1} &: |T_1\rangle = \frac{1}{\sqrt{2}}(-|\alpha\alpha\beta\beta\rangle + |\beta\beta\alpha\alpha\rangle),\\
\text{Triplet 2} &: |T_2\rangle = \frac{1}{\sqrt{2}}(-|\alpha\beta\alpha\beta\rangle + |\beta\alpha\beta\alpha\rangle),\\
\text{Triplet 3} &: |T_3\rangle = \frac{1}{\sqrt{2}}(-|\alpha\beta\beta\alpha\rangle + |\beta\alpha\alpha\beta\rangle),\\
\text{Quintet} &: |Q\rangle = \frac{1}{\sqrt{6}}\,(|\alpha\alpha\beta\beta\rangle + |\beta\beta\alpha\alpha\rangle + |\alpha\beta\alpha\beta\rangle + |\beta\alpha\alpha\beta\rangle + |\alpha\beta\beta\alpha\rangle + |\beta\alpha\beta\alpha\rangle).
\end{aligned}
\qquad 5.
$$

Here, the numerical subscript counts the different singlet ($n = 1, 2$) and triplet ($n = 1, 2, 3$) states, and $|\alpha\rangle$ and $|\beta\rangle$ are the standard one-electron spin states. We have omitted any four-electron superscripts for simplicity, although we continue to use superscripts for the two-electron states to differentiate them.

The singlet and quintet wave functions presented here are identical to those in References 2, 3, 23, and 24. However, where reported, the triplet wave functions differ (2). We discuss $|T_n\rangle$ below, concentrating for now on $|S_n\rangle$ and $|Q\rangle$. Provided that orbital overlap between the two sites is weak, $|S_n\rangle$ and $|Q\rangle$ can be written as pairs of excitations (2, 10, 22). For example, the first singlet state can be written as combinations of triplet excitations: $|S_1\rangle \approx \frac{1}{\sqrt{3}}(|00\rangle - |{+}{-}\rangle - |{-}{+}\rangle)$ in the high-field basis (Equation 1) [or equivalently $|S_1\rangle \approx \frac{1}{\sqrt{3}}(|xx\rangle + |yy\rangle + |zz\rangle)$ in the zero-field basis (Equation 3)]. This singlet state is therefore described as a correlated pair of triplets, denoted ^{1}(TT). $|S_2\rangle$ can similarly be written as a pair of singlets ^{1}(SS). Likewise, $|Q_{M_S=0}\rangle \approx -\frac{1}{\sqrt{6}}(|{+}{-}\rangle + |{-}{+}\rangle + 2\,|00\rangle)$ shows that the quintet is also described as a correlated triplet pair: ^{5}(TT). Therefore, ignoring wave function overlap or intertriplet spin-dipolar coupling (discussed below), $|S_1\rangle = {}^1$(TT) and $|Q\rangle = {}^5$(TT) are degenerate at an energy $2E_T$. Compared with these, $|S_2\rangle = {}^1$(SS) lies $4J_0 \sim 1$–2 eV higher in energy (**Figure 1*d*,*e***) [J_0 is the intrapair exchange energy, defined as half the two-electron singlet-triplet energy gap (see **Figure 1*b***)].

Despite the use of similar methods of constructing the four-electron basis set, the three $S = 1$ triplet states—$|T_1\rangle$, $|T_2\rangle$, and $|T_3\rangle$—have been described differently in early work by Kollmar (22), reproduced in Equation 5, and more recent work by Scholes (2). According to Scholes (2) (**Figure 1*d***), $|T_3\rangle$ is a correlated triplet-singlet pair, ^{3}(TS), while $|T_1\rangle$ and $|T_2\rangle$ comprise explicit singlet-triplet pair contributions as well as a linear combination of triplets that is an overall triplet state. The presence of ^{3}(TS) in all the $|T_n\rangle$ states lifts the degeneracy between $|S_1\rangle$ and $|T_n\rangle$, as shown in **Figure 1*d***. Scholes calculates that the smallest $|S_1\rangle - |T_1\rangle$ diabatic energy gap to first order is $\frac{2}{3}J_0$. In singlet-fission-based systems, it has typically been found that $J_0 \sim 0.5$ eV and J_0 should dominate over any other intertriplet interaction terms.

In contrast to Scholes's analysis, Kollmar (22) (**Figure 1*e***) used a very similar construction of the four-electron basis set but concluded that $|T_1\rangle$ is a correlated triplet pair, ^{3}(TT), with no discernible singlet-triplet contribution. Both $|T_2\rangle$ and $|T_3\rangle$ are described as correlated singlet-triplet pairs ^{3}(TS), with energy $E_S + E_T$, shown in **Figure 1*e***. The result of Kollmar's description is that $|T_1\rangle$ is degenerate with both $|Q\rangle$ and $|S_1\rangle$. In Kollmar's case, all three of the lowest-lying four-electron states can be described as pairs of triplets. All nine of the possible such triplet pairs, including $M_S \neq 0$ states, are described in Merrifield's (25) classic work in both triplet-product bases.

The difference between Scholes's (**Figure 1*d***) and Kollmar's (**Figure 1*e***) analyses appears to stem from the method of antisymmetrizing the total wave function. Kollmar emphasized the fact that the triplet and singlet states require wave functions that are a sum of products of orbital and spin contributions (26). The discrepancy in predicting the diabatic $|T_1\rangle$-$|S_1\rangle$ energy gap has important consequences for understanding the triplet-pair states and exploiting them. For example, the maximum achievable yield of upconversion from triplet-triplet annihilation depends on the relative position of $|T_1\rangle$. Likewise, analysis of magnetic-field-dependent fluorescence and of electron paramagnetic resonance (EPR) spectroscopy requires knowledge of the relative position of the low-lying $|T_1\rangle$ levels (27–31). Recent magnetic-field-dependent fluorescence measurements have been interpreted to suggest that $|T_1\rangle$ lies very close ($\leq$10 meV) to $|S_1\rangle$ (28–31).

2.3. Fine Structure of the Lowest-Lying Four-Electron States

Having described the coarse electronic structure of the four-electron states, we move on to consider the fine structure, which, as discussed in Section 3.4, is important to understand the dynamic behavior of triplet-pair states. In the absence of nonadiabatic coupling and geometric molecular reorganization, the fine structure of four-electron states is described by the total spin Hamiltonian. This is shown below for four electrons at sites A and B in the absence of spin-orbit coupling (32–35):

$$\hat{H}_{\text{spin}} = \sum_{i=A,B} \underbrace{g_i \mu_B \mathbf{B} \cdot \hat{\mathbf{S}}_i}_{\text{Zeeman}} + \underbrace{D_i \left(\hat{S}_{i,z}^2 - \hat{\mathbf{S}}_i^2/3 \right) + E_i \left(\hat{S}_{i,x}^2 - \hat{S}_{i,y}^2 \right)}_{\text{Intratriplet dipolar}} + \underbrace{\hat{\mathbf{S}}_A \cdot D_{\text{inter}} \cdot \hat{\mathbf{S}}_B}_{\text{Intertriplet dipolar}} + \underbrace{J \hat{\mathbf{S}}_A \cdot \hat{\mathbf{S}}_B}_{\text{Exchange}}. \quad 6.$$

Here g_i are the g factors of the electrons on sites $i = A, B$; μ_B is the Bohr magneton; $\mathbf{B}$ is the external magnetic field; D_i and E_i are the on-site zero-field parameters defined in Equation 4; $\hat{\mathbf{S}}_A \cdot D_{\text{inter}} \cdot \hat{\mathbf{S}}_B$ can be formulated in different ways, depending on how the intertriplet geometry and exchange interactions are accounted for (32–35); and it can be approximated to $D_{AB}(\hat{\mathbf{S}}_{A,z}\hat{\mathbf{S}}_{B,z} - \hat{\mathbf{S}}_A\hat{\mathbf{S}}_B/3)$ (32), where D_{AB} is the intertriplet dipolar coupling, and the spin operators are given by

$\hat{\mathbf{S}}_A = \hat{\mathbf{S}}_1 + \hat{\mathbf{S}}_2$ and $\hat{\mathbf{S}}_B = \hat{\mathbf{S}}_3 + \hat{\mathbf{S}}_4$. In molecular systems such as tetracene, recent measurements suggest that the intertriplet D_{AB} is approximately 10 neV (21, 33), compared with intratriplet $D_i \sim 10$ μeV. The E values are often set to zero for symmetric molecular systems as $E \ll D$ (21, 32, 36). J is the exchange coupling term, which is currently thought to vary between 0 and 5 meV (23, 28).

In this equation, the exchange term (J) is mediated by bond or orbital overlap, while the spin-dipole terms (D_{AB}, E_{AB}) are considered as a through-space interaction. A bond-like interaction requires orbital overlap and can be described using configuration interaction (22), for example, by mixing between charge-transfer ^{1}(CT), ^{3}(CT) states, and correlated triplet-pair states $|S_1\rangle$, $|T_1\rangle$. Since it is not possible to have charge-transfer states with $S = 2$ of comparable energy, $|Q\rangle$ does not mix with other states in the absence of spin mixing. Therefore, ignoring nonadiabatic effects and geometric molecular relaxation, its energy remains at that of two free triplets, defined as $2E_T$ (**Figure 1*e***). On the other hand, $|S_1\rangle$ and $|T_1\rangle$ are stabilized through the configuration interaction.

As an example of how the configuration interaction relates to the exchange term in Equation 6, and how we can use this to describe the relative energies of $|S_1\rangle$, $|T_1\rangle$, and $|Q\rangle$, let us consider the case described in Reference 22. In this case, the triplet-pair states mix with a charge-transfer state where transfer between orbitals 1 and 3 (see **Figure 1*b***) is governed by the transfer integral t_{13}. By second-order perturbation theory (assuming $|t_{13}| \ll |J_0|$), the energy differences between $|S_1\rangle$, $|T_1\rangle$, and $|Q\rangle$ are given by $2\Delta E_{ST} = \Delta E_{QT} = t_{13}^2/(U_{13} + J_0)$. Here U_{13} is the Coulomb repulsion between electrons in orbitals 1 and 3, and J_0 is the exchange energy, defined as half the two-electron singlet-triple gap (**Figure 1*c***). The state ordering becomes $E_{|S_1\rangle} < E_{|T_1\rangle} < E_{|Q\rangle}$.

This energetic splitting is characteristic of the exchange coupling J, when taking $J = -t_{13}^2/2(U_{13} + J_0)$. The energetic spacing becomes $\Delta E_{ST} = 2J$ and $\Delta E_{QT} = 4J$, as depicted in **Figure 1*e***. This energy splitting ratio is used to describe exchange coupling between triplet-pair states in the literature, particularly in relation to spin resonance spectroscopy or magnetic-field effects discussed in Section 3.4 (27–31, 36, 37).

The fine-structure splitting between sublevels and stabilization relative to $2E_T$ is likely to be more complex than that described here. It will include, for example, mixing between $|S_1\rangle$ and $|S_1^{(2)}\rangle$ that should stabilize $|S_1\rangle$ relative to $|T_1\rangle$ and $|Q\rangle$, and mixing with different charge-transfer states (34). [We recall that throughout $|S_1\rangle$ denotes the four-electron singlet ($S = 0$), while $|S_1^{(2)}\rangle$ denotes the two-electron singlet.] The simple description here also ignores nonadiabatic coupling and geometric relaxation, which has been suggested (38–40) to be substantial (~0.5 eV).

Following theory developed by Benk & Sixl (35), there are two limiting cases when considering the relative magnitudes of the exchange and dipolar coupling terms: The first case involves mixed-spin states, where $J \to 0$ due to negligible orbital overlap between sites. This means that $\Delta E_{SQ} \approx 0$. In this case, the dipolar terms D_{AB} dominate, allowing mixing between $|S_1\rangle$ and $|Q\rangle$ to produce mixed $|SQ\rangle$ states, described in Reference 35. Note that, in the case of identical triplets, $|T_1\rangle$ does not mix with $|S_1\rangle$ or $|Q\rangle$ due to symmetry. The second case involves pure spin states, where J is sufficiently large such that $\Delta E_{SQ} \gg D$. In this case, the different spin states cannot mix and remain pure $|S_1\rangle$ and $|Q\rangle$.

Historically, the existence of mixed-spin states where $\Delta E_{SQ} \approx 0$ was assumed in Merrifield's (25) and Suna's (41) models of triplet-triplet annihilation. These models provide excellent predictions for <1 T magnetic-field delayed fluorescence measurements and, with the inclusion of coherence (7), quantum beating. At the other extreme, pure spin states with significant configuration interaction and $\Delta E_{SQ} \gg D$ are known to occur in polyenes. In polyenes, the lowest-lying singlet state, denoted 2Ag, is described by various configurations, the largest of which is a four-electron spin-0 triplet-pair state, $|S_1\rangle$ (42). This state is known to be significantly mixed with

charge-transfer components and $S_1^{(2)}$ (39, 43). In addition, 2Ag is known to be stabilized by ~1 eV through geometric reorganization (38, 39). In short-chain polyenes such as all-*trans* β-carotene, experimental observations of the adiabatic $|S_1\rangle$ state suggest that it behaves as expected for a pure singlet state. For example, although symmetry forbidden, the nonradiative decay from $|S_1\rangle$ is very rapid, suggesting no need for spin mixing. Similarly, emission from $|S_1\rangle$ is observed through a Herzberg–Teller mechanism (44, 45). Such emission has been observed in free jet expansions with incredible spectral resolution (45). These experiments demonstrated that the pure electronic 0-0 emission is absent. Instead, emission originates from a false origin due to odd-symmetry Herzberg–Teller promoting modes. These experiments demonstrate that if pure triplet-pair states with significant ΔE_{SQ} exist, their emission spectra should have a weak 0-0 emission.

3. RECENT EVIDENCE FOR BOUND TRIPLET-PAIR STATES

The Merrifield (25, 46) model of triplet-triplet annihilation and singlet fission developed in the 1970s, which assumes $\Delta E_{SQ} \sim 0$ and an unbound or weakly bound ^{1}(TT) state with mixed-spin character, has been very successful in describing steady-state or delayed fluorescence measurements with or without an applied magnetic field. However, with technological advances in time-resolved optical and spin resonance spectroscopy, and the new observations these have enabled, the concept of a bound—and therefore pure spin—triplet-pair state has been invoked in recent years.

3.1. Identification of ^{1}(TT)

At first the concept of a bound ^{1}(TT) was used to resolve controversy over the interpretation of ultrafast time-resolved measurements in pentacene thin films. This debate has previously been reviewed elsewhere (4, 5), but we highlight that computational (47) and experimental (48) studies claimed evidence of a distinct multiexcitonic (2Ag-like) ^{1}(TT) state intermediate to singlet fission. Both results proved highly controversial (4, 5, 49, 50) but inspired deeper investigation into the possible nature of ^{1}(TT).

More recently, to explain the surprising lack of a temperature dependence in the measured rate of singlet fission in polycrystalline tetracene films, which is expected to demonstrate endoergic singlet fission [$(2E_T - E_S) \approx 250$ meV], Burdett et al. (51) and Tayebjee et al. (52) tentatively proposed that singlet fission proceeds through a lower-energy intermediate state. They described this state as weakly emissive and potentially exhibiting triplet-pair character reminiscent of the 2Ag state in polyenes.

Following this, the role of an intermediate ^{1}(TT) state to mediate endothermic singlet fission was explicitly invoked in 2015 to describe the photophysics of concentrated TIPS-tetracene solutions (53). Transient absorption measurements showed evidence of efficient singlet fission through a diffusional mechanism (54), despite being endoergic by ~250 meV. In the transient absorption measurements, the intermediate state showed triplet-like absorption features on a broad background. These features were directly correlated with excimer emission dynamics. The authors assigned the intermediate state as an emissive, bound pair of triplets, ^{1}(TT), that was proposed to be an essential intermediate in endothermic singlet fission. This interpretation has proved controversial, however, with others proposing a branching decay pathway from $S_1^{(2)}$ either into excimers with no ^{1}(TT) character or directly into free triplets (55). This debate notwithstanding, the optical assignment of a bound ^{1}(TT) intermediate in singlet fission has inspired numerous subsequent studies.

In the solid state, two ultrafast vibrational spectroscopy studies on pentacenes (56, 57) hinted at the existence of an intermediate state that evolved into free triplets. A similar model was also invoked in a much wider range of experimental systems, including covalent dimers (58), acene nanocrystals (59, 60) and thin films (6, 58, 61, 62), but with ambiguous and often contradictory definitions of ^{1}(TT). Properties of this state such as its lifetime, excited-state structure, and energetic position with respect to its parent singlet $S_1^{(2)}$ (energy E_S) and a pair of free triplets (energy $2E_T$) remained unclear.

A series of three studies teased apart detailed temperature-dependent transient absorption and emission data in 2017 to provide a more comprehensive description of the intermediate state and its role in thin films (63–65). They showed, in polycrystalline films of a range of acenes (63, 65), heteroacenes (65), and diradicaloid zethrenes (64), that the intermediate state can be identified as ^{1}(TT). Regardless of whether singlet fission is endoergic [$E_S < 2E_T$] or exoergic [$E_S > 2E_T$], the ^{1}(TT) state is energetically bound with respect to both its parent two-electron $S_1^{(2)}$ and free triplets, and as a singlet state it is capable of direct (symmetry-forbidden) emission analogous to the polyene 2Ag state. Strikingly similar emission is also observed in defect-free single crystals of pentacene (66). We briefly describe here the evidence used to justify these claims, described in more detail in the following sections.

1. The prompt $S_1^{(2)}$ emission (**Figure 2*a***) decays with the same time constant as the initial $S_1^{(2)}$ excited-state absorption features in transient absorption (**Figure 2*b***) (63–65). This process is temperature independent in all tested polycrystalline systems (51, 52, 63–65, 67), showing that $E_S > E_{1_{(TT)}}$.
2. Following $S_1^{(2)}$ decay, a new red-shifted emissive species can be observed (**Figure 2*a***) (63–65). The spectra typically exhibit well-resolved vibronic structure inconsistent with excimer emission (see examples in Section 3.2). The emission dynamics of this state are closely correlated with a second state observed in transient absorption (**Figure 2*b***) (64, 65), as demonstrated by comparing the respective transient absorption and photoluminescence dynamics

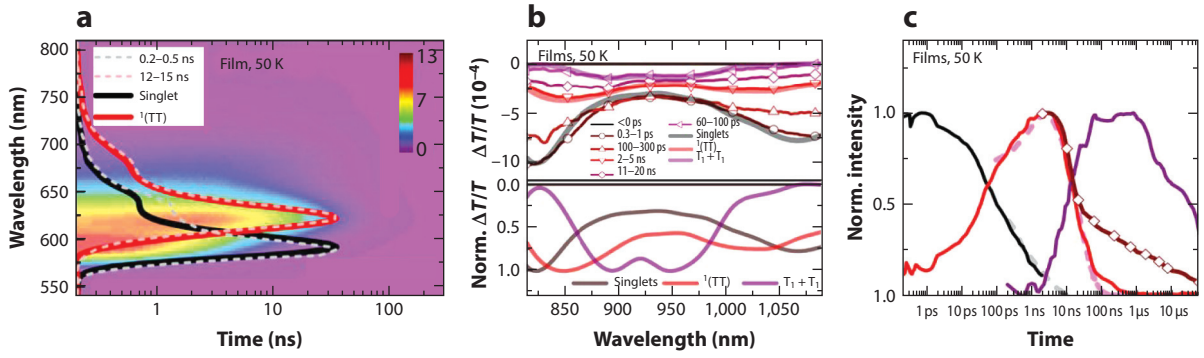

Figure 2

Identification of intermediate ^{1}(TT) in F_2-TES ADT film. (*a*) Transient photoluminescence reveals distinct prompt (*black*) and delayed (*red*) emitting species. The rise of the delayed emitter can be directly resolved. (*b*) Low-temperature transient absorption shows conversion from $S_1^{(2)}$ (*black*) to free triplets $T_1 + T_1$ (*purple*). The distinct species on intermediate timescales (*red*) can be identified as ^{1}(TT). (*c*) Species population kinetics extracted from transient absorption (*solid lines*) show clear sequential progression and closely track those from transient photoluminescence (*dashed lines*). The intermediate ^{1}(TT) is thus emissive. The raw transient absorption kinetic (*diamonds*) tracks both triplet-related species. Figure adapted from Reference 65, licensed under a Creative Commons Attribution 4.0 International License.

in **Figure 2*c***. The absorption spectrum of this intermediate state is distinct from free triplets (**Figure 2*b***) (63–65).

3. The presence of this red-shifted emissive state coincides with quantum beating in the delayed emission (64, 65), demonstrating that—at least during this initial decay—the system contains triplet pairs with correlated spin (33, 68, 69) (see Section 4).
4. The decay of the second state results in the formation of identifiable free triplets with long lifetimes (e.g., **Figure 2**) (63–65), with the exception of isolated cases where no free triplets can be identified (63–65).
5. The formation of free triplets from the intermediate state is temperature dependent to a varying degree in all materials, providing evidence that $E_{^1(TT)} < 2E_T$ (63–65). The intermediate state is therefore also bound with respect to free triplets.
6. The pure electronic emission energy (i.e., 0-0 emission energy) of the intermediate species closely tracks $2E_T$, with an offset (64, 65) (Section 3.2). At the same time, the intermediate state can show distinct triplet-like excited-state absorption fingerprints (63, 64) (Section 3.3).

Together, these points identify an intermediate state in singlet fission and assign it to ^{1}(TT). They show that ^{1}(TT) is bound with respect to both its parent two-electron singlet state $S_1^{(2)}$ (energy E_S) and a pair of free triplets (energy $2E_T$) and, as we describe further below, is common to all singlet-fission systems studied to date.

Having demonstrated the existence of ^{1}(TT), we now look to describe its properties. We start by defining the binding energy of ^{1}(TT) as $E_b = 2E_T - E_{^1(TT)}$. Then, assuming the quintet energy is equal to $2E_T$ (3), we see from **Figure 1** that $E_b = \Delta E_{SQ} = 6J$. In other words, in the absence of stabilization of $|Q\rangle$ [which might occur through geometrical reorganization (40) or nonadiabatic coupling (18)], ΔE_{SQ} is equal to $6J \approx$ 20–200 meV (Section 3.2). This large separation would prevent mixing between $|S_1\rangle$ and $|Q\rangle$, suggesting that ^{1}(TT) must be a pure spin state similar to 2Ag in carotenoids and other polyenes (Section 2.3). To test this conclusion, we now consider the photophysical and spin properties of ^{1}(TT) in more detail to determine whether ^{1}(TT) is a pure spin-singlet state and, if so, whether it behaves like the 2Ag state in polyenes.

3.2. Emission Spectra of ^{1}(TT)

One of the most surprising findings in the studies described above is that ^{1}(TT) is not a completely dark state but can emit photons (63–65). Because its decay is kinetically distinct from $S_1^{(2)}$, the ^{1}(TT) emission spectrum can be isolated with spectral decomposition, as shown in **Figure 2*a***. Strikingly similar delayed emission spectra have been extensively studied in tetracene (51, 52, 70) (**Figure 3*b***) and even observed in high-quality pentacene films (71) (**Figure 3*c***) and single crystals (66). The temperature dependence reveals stark differences between prompt and delayed emissive species. At low temperatures, the prompt singlet emission typically exhibits strong enhancement of the 0-0 peak, due to a reduction in disorder that leads to greater delocalization and consequently superradiance (52, 65, 67, 71, 72). The ^{1}(TT) emission spectral shape, by contrast, is largely temperature independent (52, 64, 65, 71). This behavior is indicative of a state that is highly localized regardless of disorder, as might be expected for a triplet pair. We note that the 2Ag state in xanthophyll carotenoids shows similar temperature-independent behavior (44).

The most obvious question inspired by these spectra is simply, How can this nominally dark, multiexcitonic state emit? As noted in Section 2.3, in polyenes emission from 2Ag occurs through a Herzberg–Teller mechanism, where coupling to an odd-symmetry vibration breaks symmetry, allowing the radiative transition. In analogy, we might expect that ^{1}(TT) should emit through a

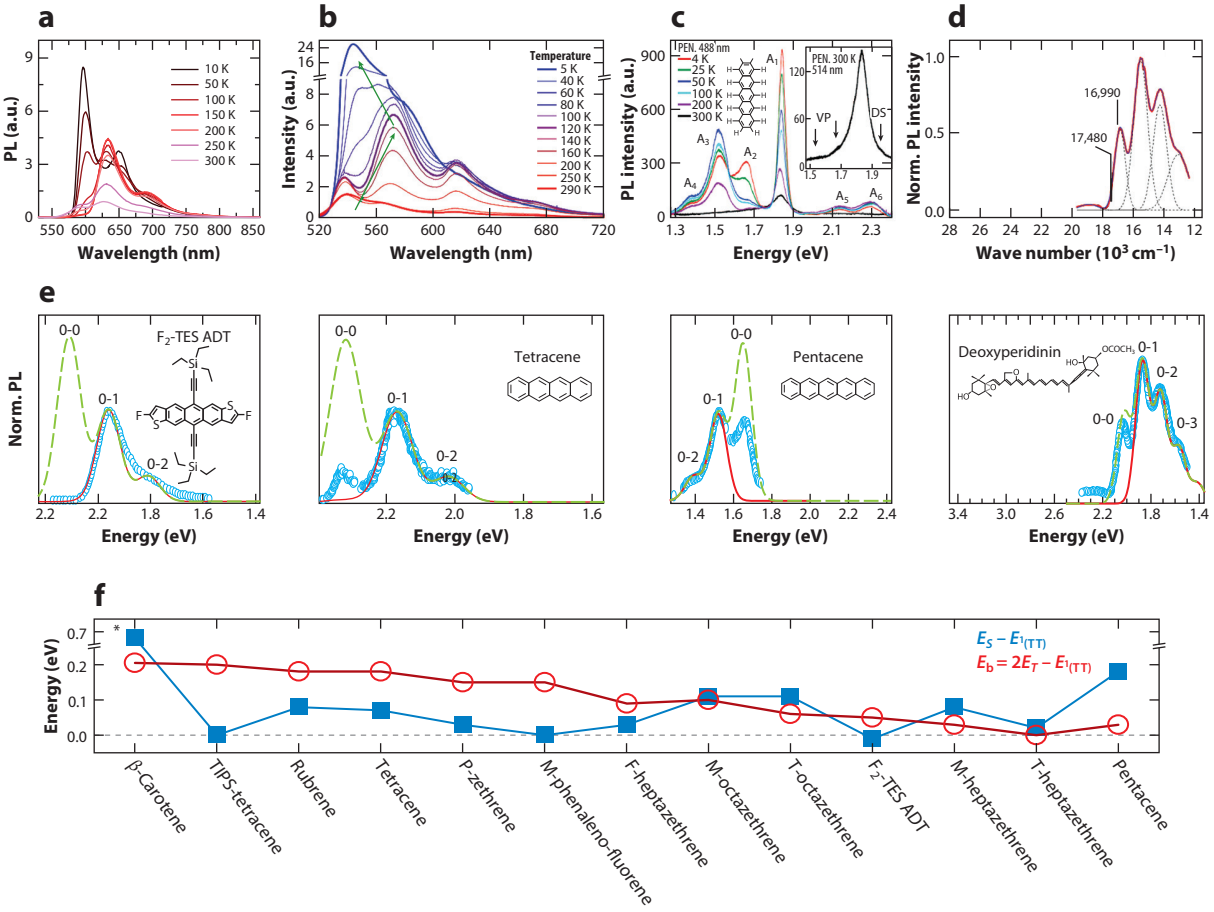

Figure 3

Emission from ^{1}(TT). Photoluminescence in polycrystalline films of (*a*) F_2-TES ADT, (*b*) tetracene, and (*c*) pentacene, revealing a vibronically structured subgap species enhanced at low temperature. This feature coincides with ^{1}(TT) in transient absorption. (*d*) For comparison, absorption (*black*) and emission (*red*) spectra of carotenoid deoxyperidinin at 77 K. Vibronically structured emission is primarily from 2Ag in this carotenoid. (*e*) Extracted ^{1}(TT) (F_2-TES ADT, tetracene, pentacene) or 2Ag (deoxyperidinin) emission (*circles*), which can be fitted with a Franck–Condon progression (*red curves*), allowing extrapolation of the ^{1}(TT) 0-0 peak (*dashed/green curves*). The tetracene spectrum is taken from Reference 51, and the others are from the panels above. Details of the fits are available in Reference 65, except for deoxyperidinin, where the Huang–Rhys parameter is $S = 2$, the effective vibrational energy is 0.153 eV, $E_{0\text{-}0} = 2.02$ eV, and Gaussian widths are kept constant for the different vibronic replicas at 0.08 eV. The red curves have 0-0 artificially set to zero, while the dashed/green curves show the expected 0-0 intensity in the absence of symmetry-induced suppression. (*f*) The stabilization of ^{1}(TT) versus $S_1^{(2)}$ and $2E_T$, based on reported energy measurements. ^{1}(TT) is in all cases lower in energy than $2E_T$. In systems where ^{1}(TT) is approximately isoenergetic with $S_1^{(2)}$ (e.g., TIPS-tetracene, F_2-TES ADT), significant delayed fluorescence is observed (63, 65). Materials are as follows: β-carotene (77, 78) [note here that $S_1^{(2)} = 1$Bu and ^{1}(TT) = 2Ag], TIPS-tetracene (63), rubrene (65), tetracene (51, 52, 65, 67), P-zethrene (64), M-phenaleno-fluorene (64), F-heptazethrene (64), M-octazethrene (64), T-octazethrene (64), F_2-TES ADT (65), M-heptazethrene (64), T-heptazethrene (64), and pentacene (65, 66, 71). Zethrene solubilizing units are triisopropylsilylethynyl (T, TIPS), mesityl (M), fluorinated mesityl (F), and phenylethynyl (P). Panel *a* adapted from Reference 65, licensed under a Creative Commons Attribution 4.0 International License. Panel *b* adapted with permission from Reference 67; copyright 2013 American Chemical Society. Panel *c* adapted from Reference 71, with permission from AIP Publishing. Panel *d* adapted with permission from Reference 74; copyright 2016 American Chemical Society.

similar symmetry-breaking mechanism. This turns out to be the case. Calculations for F_2-TES ADT (65) show that emission requires the presence of a symmetry-breaking molecular distortion as well as coupling to $S_1^{(2)}$. This is equivalent to Herzberg–Teller coupling. Interestingly, two-dimensional electronic spectroscopy on acene films has also uncovered the reverse process: Through coupling to vibrational modes, the ^{1}(TT) state can mix with bright $S_1^{(2)}$ and acquire weak oscillator strength (57).

One of the key implications of emission via Herzberg–Teller coupling is that the 0-0 peak should be suppressed in the absence of significant disorder (45, 73). Thus, to extract the energy of ^{1}(TT) from the emission, we cannot simply read off the origin of the first spectral peak but must instead consider the vibronic progression. As shown in **Figure 3*e***, the most prominent peak in the (hetero)acene spectra can be treated as the 0-1 emission. Fitting to that and the next (0-2) peak with a standard Franck–Condon progression gives the spacing between peaks, and an estimate of the Huang–Rhys parameter, allowing extrapolation of where the suppressed 0-0 peak should be.

Direct comparison of these spectra with polyene systems is difficult as similar analysis has not been explicitly performed on polyenes in the condensed phase (44, 74, 75). This is because, in contrast to the gas phase (45), polyene or carotenoid emission spectra are overlapped with $S_2^{(2)}$ emission and broadened due to strong coupling to low-energy vibrational modes and conformational disorder (44). However, recent measurements on deoxyperidinin at 77 K (74) show clear, structured 2Ag emission (**Figure 3*d*,*e***). In this case, a Franck–Condon fit to the 0-1, 0-2, and 0-3 vibronic replica demonstrates that the 0-0 peak is only slightly suppressed, as well as being slightly blue-shifted compared with the expected position. That 0-0 is not totally suppressed is probably due to molecular disorder, as discussed in Reference 76. Although we do not expect such large disorder in polycrystalline (hetero)acene films, in some instances the 0-0 peak is still only partially suppressed. This is exemplified in pentacene at low temperatures (**Figure 3*c***) (66, 71). As the effect of disorder should reduce as the temperature is lowered, the increased ^{1}(TT) 0-0 emission is instead tentatively linked to the evident superradiance (i.e., strong enhancement of 0-0) of the bright $S_1^{(2)}$, which may partially counteract the 0-0 suppression in ^{1}(TT).

In all cases, the position of the 0-0 peak can be taken as the approximate energy of the state. It is reassuring that this energy tracks the $2E_T$ energy rather than E_S. This behavior is clearest in zethrenes (64) and pentacene (66, 71), where the emission is substantially red-shifted from that of $S_1^{(2)}$. This is observable even in defect-free single crystals (66). Such emission is currently the most direct method of determining the energy of ^{1}(TT). Using this energy, **Figure 3*f*** shows that in every reported system (63–65), $E_{^1(\mathrm{TT})} < 2E_T$, similar to polyenes (77, 78). A cautionary note is in order regarding the interpretation of delayed emission spectra. We have focused the discussion on systems in which the delayed emission exhibits clear vibronic structure as optimal examples of the Herzberg–Teller model. However, in many other singlet-fission systems, the delayed emission is less amenable to detailed analysis. Tetracene, for example, is well known to exhibit broad excimer emission that partially overlaps with the ^{1}(TT) spectrum (52, 65, 67). It can also be populated by triplet-triplet annihilation, making it difficult to distinguish kinetically from ^{1}(TT). However, the excimer-forming defect sites can be eliminated through careful film processing (52, 67, 79), and in other systems, such as rubrene (65), disordered TIPS-tetracene (63), diketopyrrolopyrrole (62), and tetracene dimers (58), the overall envelope of ^{1}(TT) emission can be distinguished. In these cases, vibronic structure is absent, resulting in uncertainty in the Herzberg–Teller fitting (65). The same logic used to assign direct emission from ^{1}(TT) in thin films can be applied to certain donor-acceptor polymers capable of intramolecular singlet fission, for example, the red-shifted emission observed by Busby et al. (80) and by Hu et al. (81) in polyene-charge-transfer polymers. This emission has been theoretically analyzed based on a modified polyene framework (82), suggesting that coupling with charge-transfer states, rather than vibrations, breaks the symmetry to

allow emission. This mode of symmetry breaking could also be occurring in deoxyperidinin in **Figure 3**.

3.3. ^{1}(TT) Excited-State Absorption

The first explicit invocation of a distinct ^{1}(TT) state as an intermediate in singlet fission was primarily justified through the decomposition of transient absorption data from concentrated solutions of TIPS-tetracene (53) [see Dover et al. (55) for the controversy about this procedure]. The initial state could be identified as $S_1^{(2)}$ on isolated molecules, while the terminal state agreed with reference measurements for free triplet excitons. The intermediate state assigned to ^{1}(TT) exhibited a combination of excited-state absorption features: identifiable fingerprint peaks of the triplet, albeit slightly spectrally shifted, and a broad underlying envelope distinct from $S_1^{(2)}$ and $T_1^{(2)}$. The same basic concept—that ^{1}(TT) exhibits distinct spectral features, typically closely related to those of free triplets—is now widely applied (12, 13, 60–63, 65, 83–86), in most instances simply as a means to track the populations of different states.

However, the ^{1}(TT) excited-state absorption spectra extracted from such experiments contain far more information than this. Krylov and coworkers (40, 58, 87), for example, examined the nature of ^{1}(TT) in detail and emphasized the role of even small admixtures of singlet, charge-transfer (resonance) and other contributions to the adiabatic ^{1}(TT) wave function. These contributions affect not only the ^{1}(TT) binding energy (E_b) and the couplings with $S_1^{(2)}$ that drive singlet fission, but also the optical transitions of ^{1}(TT). A more recent consideration of tetracene films using an advanced spin-flip formalism was even able to describe the higher levels in the TT manifold, suggesting that ^{1}(TT) transient absorption signatures should be similar, though shifted, to the triplet (88). The expected shift is due to the admixture of singlet configurations within the ^{1}(TT) wave function. In contrast, Khan & Mazumdar used high-order configuration interaction calculations with the π-electron Pariser–Parr–Pople Hamiltonian to calculate the excited-state absorption of pentacene covalent dimers (89) and thin films (90). Their detailed analysis suggests that mixing of additional contributions into the ^{1}(TT) wave function completely alters the excited-state absorption spectrum (89, 90). For example, the presence of charge-transfer character in ^{1}(TT) should result in unique charge-transfer-derived transitions in the near infrared for that state, as are indeed observed (12, 60, 65, 91–93). While the full interpretation of such transient absorption spectra remains controversial, this technique demonstrates the power of excited-state absorption analysis to understand the nature of ^{1}(TT).

Important qualitative effects can also be inferred from a purely experimental perspective, especially when ^{1}(TT) spectra are collected for series of molecules with slight structural differences. An excellent case is the family of acene dimers reported by Campos and coworkers (91, 94, 95), examples of which are reproduced in **Figure 4**. In these, pentacenes or tetracenes are linked at the 2, 2′ position (effectively end to end), either directly or with a variable number of phenyl spacers. In the most closely spaced dimers (BP0 and BP1 in **Figure 4**), the triplets formed by singlet fission exhibit significant differences from those generated through triplet sensitization (where a single triplet sits on the molecule) (91, 94, 95). The new peak in the near infrared in BP0 and BP1 is related to the charge-transfer character discussed by Khan & Mazumdar (89). Increasing the number of phenyl spacers reduces the difference between sensitized and fission-generated triplet spectra. At the same time, the lifetime of the triplets formed increases (91, 94, 95). It therefore appears reasonable to correlate the degree of difference between sensitized and fission-generated triplets with the strength of interaction or binding within the triplet pair, consistent with the original proposal from TIPS-tetracene solutions (53). This behavior is representative of the vast majority of reported acene dimers (12, 37, 58, 96–103).

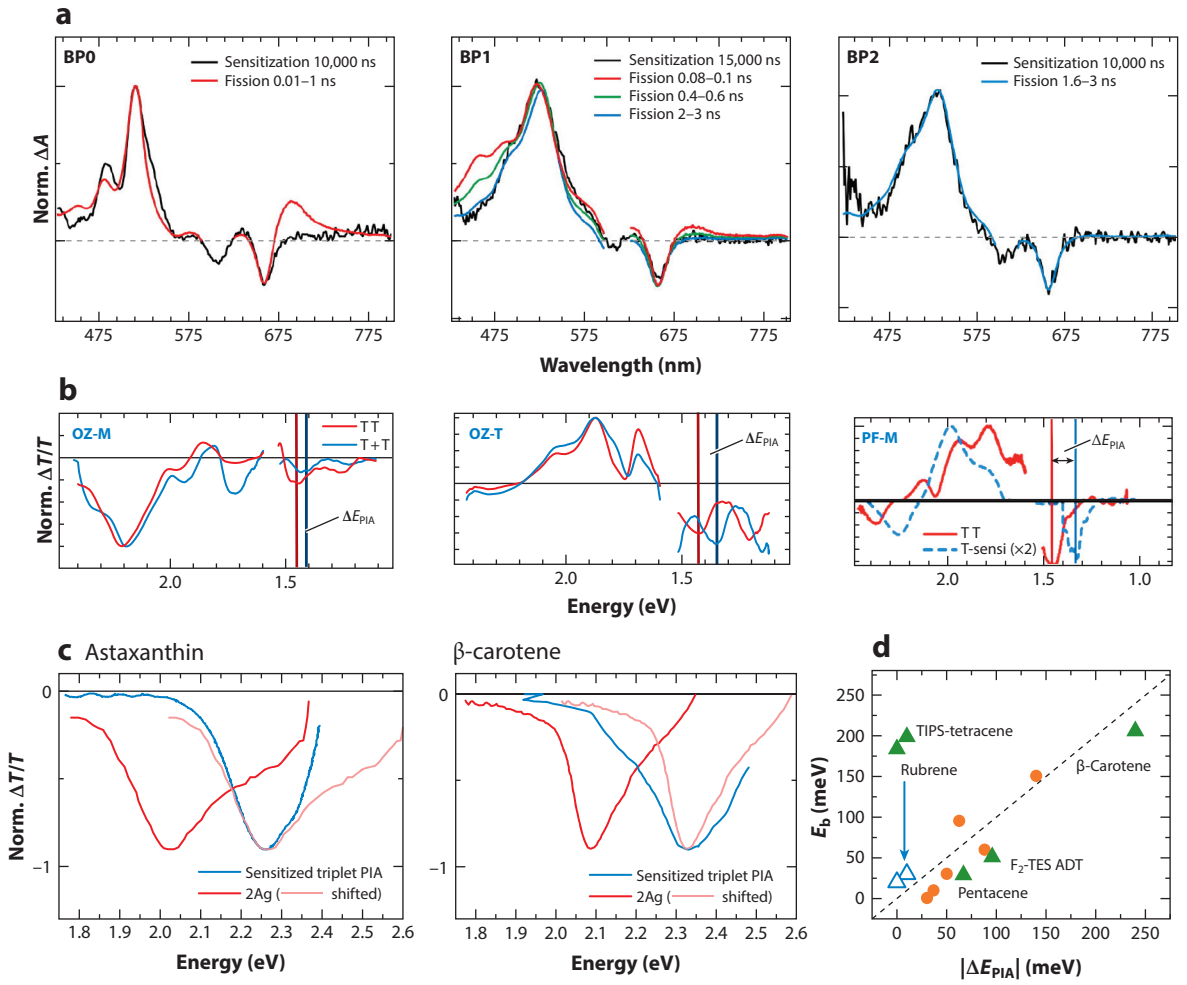

Figure 4

^{1}(TT) excited-state absorption spectra. (*a*) Transient absorption spectra of 2,2′-linked pentacene dimers, with zero (BP0), one (BP1), or two (BP2) phenyl spacers (structures in **Figure 6**). In closely spaced dimers, fission generates interacting triplet pairs with distinct excited-state absorption. Panel *a* adapted with permission from Reference 91; copyright 2015 American Chemical Society. (*b*) Excited-state absorption bands of mesityl-octazethrene (OZ-M), TIPS-octazethrene (OZ-T), and mesityl-phenaleno-fluorene (PF-M), extracted from transient absorption maps in Reference 64. Vertical lines denote fingerprint peaks to identify the shift between ^{1}(TT) and T+T species. Panel *b* adapted from Reference 64, licensed under a Creative Commons Attribution 4.0 International License. (*c*) Excited-state absorption bands of astaxanthin (129) and β-carotene (104) showing sensitized triplet (*blue*) and 2Ag [$\approx^1$(TT)] at 10 ps (*red*). Astaxanthin panel adapted from Reference 129, licensed under a Creative Commons Attribution 4.0 International License. (*d*) Extracted spectral shift ΔE_{PIA} compared with ^{1}(TT) binding energy E_b (**Figure 3*f***) for all zethrenes (*orange circles*). As described in Reference 64, the two values are correlated (the *dashed line* has a slope of 1). Also shown are similar data for other materials (*filled green triangles*), where the values have been extracted from the 50-K spectrum for pentacene (65), the 110-K spectrum for rubrene (65), and room-temperature solution spectra for TIPS-tetracene (53) and β-carotene (104). We note that we were unable to determine ΔE_{PIA} for tetracene as triplets and/or ^{1}(TT) in the solid state at low temperature has vanishing excited-state absorption oscillator strength (65). Using the definition $E_b = 2E_T - E_{1(TT)}$, rubrene and TIPS-tetracene lie off the trend line. However, as shown by the open triangles, taking the ^{1}(TT) binding energy to be defined from magnetic-field-dependent measurements ($E_b = 6J$) for TIPS-tetracene, or by the activation energy ($E_b = E_a$) for free triplet formation in rubrene (Sections 3.5.1 and 3.4.1 respectively), places both materials on the trend line. The definition of ^{1}(TT) binding energy E_b is discussed in Section 3.4.2.

Aside from the theoretical work discussed above, there has been little detailed analysis of the ^{1}(TT) spectra obtained in the solid state, as they are more challenging to isolate and systematic structural studies are more demanding than in solution. A notable exception is a family of zethrene diradicaloids with different conjugation length and intermolecular packing (64). In these systems, the excited-state absorption spectra of free triplets exhibited unique fingerprint peaks in the near infrared. The same peaks could be identified in the more complex ^{1}(TT) spectra, but distinctly shifted to higher energies (see **Figure 4*b***). In this system, it was also possible to measure ^{1}(TT) emission and, together with sensitized phosphorescence, directly determine the binding energy of ^{1}(TT) [$E_b = 2E_T - E_{^1(TT)}$]. Comparison of the degree of shift ($E_{\Delta PIA}$) with E_b (**Figure 4*d***) (64) reveals a striking—almost 1:1—correlation, suggesting that when distinct peaks can be identified, their shifts can be used as a proxy for the strength of the intertriplet coupling.

We have used this methodology with values reported for other material systems (**Figure 4*d***). We note that we take the absolute values of ΔE_{PIA} as—for some as yet unknown reason—the shift is sometimes in the opposite direction to that observed for zethrenes. Interestingly the correlation holds even for β-carotene, assuming 2Ag $\approx$ ^{1}(TT), providing additional insight into the nature of the 2Ag excited-state absorption spectrum in polyenes (104). Of the measured materials, only rubrene and TIPS-tetracene fall outside the trend when defining the ^{1}(TT) binding energy as $E_b = 2E_T - E_{^1(TT)}$. However, defining the ^{1}(TT) binding energy as the activation energy for free triplet formation from temperature-dependent measurements (Section 3.5.1) (65), rather than the measured $E_b = 2E_T - E_{^1(TT)}$, puts rubrene well within the expected trend. The same is true when taking the binding energy for TIPS-tetracene from magnetic-field-dependent measurements (Section 3.4.1). We discuss the definition of the ^{1}(TT) binding energy further in Section 3.4.2.

3.4. Spin Properties of Triplet Pairs

The optical spectroscopy results presented above show that, in many systems, ^{1}(TT) is bound with respect to free triplets. In these systems, assuming that the quintet state $|Q\rangle$ takes the energy of two free triplets, $E_Q = 2E_T$, the fact that ^{1}(TT) is bound suggests that ΔE_{SQ} (defined in **Figure 1**) is not zero. Therefore, following the definition in Section 2.3, ^{1}(TT) should be a pure spin state, $|S_1\rangle$. Magnetic-field-dependent and magnetic resonance measurements have been performed to gain more insight into the spin character of ^{1}(TT) (4, 5, 10, 25, 27–31, 33, 36, 37, 69, 102, 105). For pure spin states, application of an external magnetic field alters the energies of the $M_{S\neq0}$ states of the spin-1 triplet $|T_1\rangle$ or spin-2 $|Q\rangle$ state through the Zeeman term in Equation 6. The most intuitive experiment to probe the spin states is therefore to apply a magnetic field while monitoring the delayed fluorescence intensity. As the magnetic field grows, the quintet states with $M_{S\neq0}$ move into resonance with $|S_1\rangle$, whose energy is not altered with magnetic field. In the simplest picture, at these resonances, it is expected that $\Delta E_{SQ} = 0$, and mixing between $|Q\rangle$ and $|S_1\rangle$ can occur [mixing between $|S_1\rangle$ or $|Q\rangle$ and $|T_1\rangle$ is symmetry forbidden in the absence of inequivalent triplet g factors (23, 27)]. The mixing causes dips in the measured delayed fluorescence, as the probability of delayed fluorescence is proportional to the singlet content of the wave function (i.e., the overlap $|\langle S_1|\Psi\rangle|^2$). The dips are apparent only when the triplet pairs are pure spin states at zero field, and the relative positions of the dips give an indication of the exchange term, J, of the spin Hamiltonian in Equation 6 (**Figure 1**), while the shape and depth of the dips can be modeled to provide information on the kinetic behavior of the triplet pairs and their relative orientation (27–31).

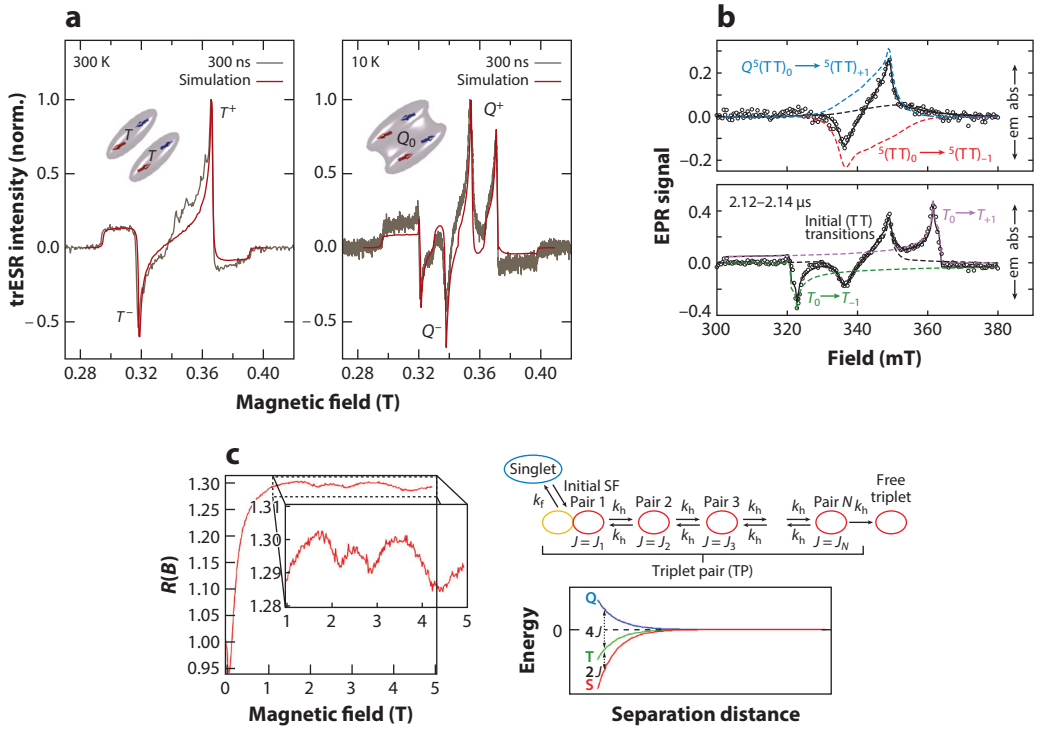

Figure 5

EPR observation of weakly interacting triplet pairs ($T^{\pm}$ or T_0) and pure spin-2 state [$Q^{\pm}$ or ^{5}(TT)] in (*a*) TIPS-tetracene and (*b*) pentacene dimer BP3. (*c*) Magnetic-field effects on the fluorescence of a diphenylhexatriene crystal, revealing distinct dips from level crossings, and the spin-correlated triplet-pair model used to simulate the level crossings. Note the explicit variation of ΔE_{SQ} during separation. Abbreviations: EPR, electron paramagnetic resonance; SF, singlet fission; trESR, time-resolved electron spin resonance. Panel *a* adapted from Reference 36 with permission from Springer Nature; copyright 2016. Panel *b* adapted from Reference 37 with permission from Springer Nature; copyright 2016. Panel *c* adapted with permission from Reference 30; copyright 2015 American Chemical Society.

3.4.1. Measurements under high (>1 T) magnetic field suggest strongly bound ^{1}(TT).

Most of the early measurements of magnetic-field-dependent delayed fluorescence observed no dips. Instead, the observed effects could be fully described by the Merrifield model discussed in Section 2.3, which assumes $\Delta E_{SQ} \approx 0$ and mixed-spin states (4, 5, 10, 25, 33, 69, 105). These measurements were performed at magnetic fields at or below ~1 T.

However, more recent high-field (>1 T) studies of diphenylhexatriene by Yago and colleagues (29–31) and TIPS-tetracene by Bayliss et al. (28) demonstrated distinct dips in the magnetic-field-dependent delayed fluorescence due to the level crossings (**Figure 5*c***). The resonance positions can be directly related to *J*, the exchange term in Equation 6 (see **Figure 1**), which was found to be on the order of 0.08–6 meV for diphenylhexatriene (29–31) and 0.3–5 meV for TIPS-tetracene (28).

3.4.2. Ambiguous definitions of the ^{1}(TT) binding energy E_b. Taking $E_b = 6J$, as is often assumed (35) (see **Figure 1** and Section 2.3), and using the reported values of *J* (28–31) give $E_b^{\text{exchange}} \approx 0.5$–30 meV. These values are small compared with those determined in **Figure 3*f*** from optical spectroscopy [$E_b^{\text{optical}} = 2E_T - E_{1(TT)} \approx$ 20–200 meV]. For TIPS-tetracene, both

have been determined (28, 53, 63), with $E_b^{optical} \approx 6E_b^{exchange}$. Interestingly, taking $E_b = 6J \approx 30$ meV matches the trend in **Figure 4*d***, as expected if ΔE_{PIA} is related to the intertriplet coupling strength. The reason for the difference between the two binding energy values (from optical spectroscopy and magnetic-field effects) is not yet clear. The models presented in the first sections of this review do not generally take into consideration geometric relaxation and nonadiabatic couplings (12, 18, 40, 63). Taking these into account may result in the finding that the assumption $E_Q = 2E_T$ (3) is inadequate. Instead, as shown in **Figure 1** and calculated in Reference 40, the entire TT manifold may stabilize relative to $2E_T$. This would set $\Delta E_{SQ} = 6J \ll 2E_T - E_{1(TT)}$. An alternative explanation could be that the quoted E_T for triplets in the solid state is incorrect, which is unlikely as E_T in tetracene and pentacene has been measured using several methods for pentacene (tetracene) in solution, 0.92 ± 0.03 eV (106, 107) [1.31 ± 0.04 eV (108–110)], and in the solid state, 0.86 ± 0.01 eV (111, 112) [1.25 eV (111, 113)]. Finally, it is possible that the different measurements probe different spatial regions of the film. In tetracene, for example, polycrystalline films behave very differently from single crystals in optical spectroscopy (79): How do the two sample types compare in other experiments?

Definitions of E_b aside, the high-field magnetic-field-dependent measurements show that ^{1}(TT) is a pure spin state (strongly exchange coupled) in both systems measured to date. As such, the Merrifield model no longer applies (21, 28–31). Yago et al. (29) instead described the full field dependence with the stochastic Liouville equation and explicit incorporation of intra- and intertriplet interactions, relative triplet orientation, triplet hopping, and spin correlations. A similar formalism was applied to explain the TIPS-tetracene film and crystal resonances at low temperatures (28).

3.4.3. Transient electron paramagnetic resonance reveals quintet formation. A more direct probe of the spin states of the triplet pairs generated by singlet fission is electron spin resonance (ESR) or EPR spectroscopy. EPR spectroscopy has previously been applied to study the spin sublevel distribution of triplets formed by singlet fission (114), and it provides a unique resonance profile to distinguish singlet fission from other mechanisms of triplet formation (115, 116). Moreover, in a recent breakthrough, time-resolved EPR spectroscopy measurements on thin films of TIPS-tetracene (36) and the widely separated 2, 2′-pentacene dimers BP2 and BP3 (37) revealed dynamics of the pure spin quintet state $|Q\rangle$ (**Figure 5*a*,*b***), characterized by peak spacing $D/3$, where D is the intratriplet dipole coupling term (Equation 4), and a ratio of Rabi frequencies for pure quintet and triplet states of $\sqrt{3}$. This state was previously considered to be energetically inaccessible (4), and its observation has sparked a re-evaluation of singlet-fission spin dynamics. It has subsequently been observed in several other pentacene dimers (102, 103) and even in thin films containing clusters of pentacene (117). Its observation is a direct demonstration of pure spin states, attributed explicitly to strong exchange coupling, J in Equation 6 (**Figure 1**) (36, 37, 102, 103, 117), and only one study (37) suggests observation of a mixed-spin state (T…T). Although Basel et al. (102, p. 5) observed EPR spectra consistent with pure (strongly exchange coupled) $|Q\rangle$, which requires $\Delta E_{SQ} \neq 0$, to explain their results, they suggested that the exchange coupling is small enough "that the lowest-lying quintet state ^{5}(TT) is nearly degenerate with the two lowest-lying bright states and with ^{1}(TT)." Transient EPR spectroscopy promises to provide many more new insights into the fission mechanism in the coming years, including the interchromophore geometries and the energetic and spin landscape arising from triplet-triplet interactions.

The obvious question raised by these observations of pure quintet states in EPR measurements is, How can a pure spin quintet state be formed from the initial (pure spin) singlet state? This is discussed in more detail in Section 5.

3.5. ^{1}(TT) Decay Mechanisms

Most studies that characterize a distinct ^{1}(TT) state are concerned less with the nature of the state than with how it decays. The greatest interest is in the separation of ^{1}(TT) into free triplets, the yield of which is important for solar cell applications. ^{1}(TT) separation is often denoted as $^1(TT) \rightarrow (T\ldots T) \rightarrow T_1 + T_1$, where the intermediate stage (T…T) denotes spatially separated, unbound, or weakly bound pairs of triplets that maintain spin coherence (2, 13, 29–31, 59, 60, 85, 118–120). However, in optical spectroscopy, there seems to be no measurable differences between (T…T) and $T_1 + T_1$ (60), and therefore we do not consider it explicitly in our discussion here. Whether requiring one or two steps, separation of ^{1}(TT) into free triplets is widely considered to be the dominant decay pathway of ^{1}(TT) in thin films (6, 58–65, 84–86, 119–124), although it is unlikely to be the only decay pathway. As discussed above, ^{1}(TT) can emit; therefore, it should also be able to decay nonradiatively directly to the ground state.

3.5.1. Triplet hopping. The consensus mechanism for the $^1(TT) \rightarrow T_1 + T_1$ process in thin films is hopping of one of the constituent triplets to a neighboring molecule, such that the coupling between them is weakened and they can diffuse freely, a process first explicitly invoked in tetracene dimers (58). In endoergic systems, the driving force for this process is attributed to the favorable increase of entropy on the transition from a localized pair state to two freely diffusing, separated triplets (58, 63, 125). This hopping picture is supported by temperature-dependent studies of singlet fission revealing that the triplet-pair separation process is thermally activated (63–65, 122), even in strongly exoergic ($E_S > 2E_T$) systems (64, 65, 122).

In these systems (e.g., F_2-TES ADT and TIPS-pentacene), the measured or estimated activation energies for triplet-pair separation [≈20–80 meV (65, 86, 122)] are in reasonable agreement with the ^{1}(TT) binding energies determined from emission measurements (65) (**Figure 3*f***). As these systems all exhibit significant π-π interactions, the intermolecular triplet transfer integrals are high enough that they do not limit ^{1}(TT) separation. This has been confirmed by Marcus–Levich–Jortner rate theory calculations showing that in these materials thermal activation of ^{1}(TT) separation is governed by $E_b = 2E_T - E_{1(TT)}$ (65), rather than by triplet hopping. This is not always the case, though. In systems where the triplet hopping integrals are small due to reduced π-π overlap, it is triplet hopping that limits the activation of triplet-pair separation, not E_b. This is the case, for example, in polycrystalline TIPS-tetracene, where the triplets remain bound at all temperatures (63), or zethrene films, where the activation energies for triplet-pair separation extracted from temperature-dependent transient absorption measurements are larger than those determined from emission measurements (64). In short, in the simplest formulation, $^1(TT) \rightarrow T_1 + T_1$ is controlled by the energy landscape for triplet hopping. Both the ^{1}(TT) binding energy and the intrinsic geometric barriers related to triplet hopping will contribute, and whichever is greater in a given material system is likely to dominate thermal activation.

Two additional cases reveal limitations to this simple picture. First, in isolated 2, 2′-linked pentacene dimers with two or three phenyl spacers (BP2 and BP3), a distinct temperature dependence is detected on long timescales correlated with triplet-pair separation (37). However, in these systems, the triplets are not able to hop to a neighboring molecule, and the underlying mechanism of this temperature dependence is not clear. Second, experiments suggest that disorder also plays a significant role. For example, although triplet-pair separation is strongly thermally activated at high temperatures, in polycrystalline films it is never entirely suppressed, even at 4–10 K, well below the ^{1}(TT) binding energy (65, 122). In contrast, in a single crystal of F_2-ADT (65), which exhibits very similar optical and singlet-fission properties to polycrystalline F_2-TES ADT, no free triplets could be detected below 200 K. The authors concluded that energetic disorder or a

distribution of interchromophore couplings at grain boundaries in polycrystalline films reduces the effective barrier for ^{1}(TT) separation. This points to a wider problem in the interpretation of complex singlet-fission dynamics in the solid state. The fission properties of polycrystalline films can be well described on the basis of reported single-crystal packing geometries (50), but spectroscopic measurements on single-crystalline versus polycrystalline samples often reveal completely different fission dynamics in endoergic (51, 52, 67, 79) and exoergic materials (56, 86, 118). These discrepancies are beyond the scope of this review but are a critical area for further research.

3.5.2. The ^{1}(TT) gap law of nonradiative decay. One of the central problems facing singlet-fission materials development is overcoming rapid triplet decay. This is a particularly pointed issue for intramolecular singlet fission, where the majority of the population typically decays at <1 ns (58, 80, 81, 91, 94, 96, 100, 101, 126–128), but rapid population decay is also observed in numerous intermolecular singlet-fission systems (13, 63, 64, 129). This behavior is generally defined as geminate triplet-triplet annihilation or triplet-pair recombination (with the terms used interchangeably). To understand its basis, we have approximated the rates of nonradiative decay of ^{1}(TT) from published $^1(\mathrm{TT}) \rightarrow \mathrm{T}_1 + \mathrm{T}_1$ kinetics in material systems where triplet-pair separation can be entirely suppressed such that the intrinsic ^{1}(TT) lifetime is directly obtained. These include covalent dimers (58, 91, 94, 101), polymers (80, 127), TIPS-tetracene (63), and F_2-ADT (65). We assume that $k_{\mathrm{rad}} \ll k_{\mathrm{nr}} \sim k_{\mathrm{tot}}$, since generally ^{1}(TT) emission is too weak to directly determine k_{rad}. The resulting rates are plotted in **Figure 6** according to the estimated energy of ^{1}(TT), taken as $\sim 2E_T$ unless it was directly characterized. For simplicity, we do not plot similar data previously reported on zethrenes (64) because their singlet and triplet states all behave markedly differently from nonbiradicaloid materials.

We compare these points to the nonradiative decay behavior of standard organic materials in the singlet and triplet states (**Figure 6**). These systems exhibit well-known gap-law behavior, in which the rate of nonradiative decay increases exponentially as the energy of the state decreases. The reference materials exhibit three distinct gap-law regimes: The polyene 2Ag singlet state has the fastest decay rate, while singlet states in isolated acenes and carbon nanotubes exhibit substantially longer lifetimes. This is related to their conformational rigidity. Isolated triplet excitons also follow a well-defined gap law, with much longer lifetimes due to the spin-forbidden nature of the transition.

We see that ^{1}(TT) nonradiative decay exhibits a wide range of behaviors. We can rationalize the full set of singlet fission materials through the simple framework of triplet-triplet interactions within ^{1}(TT). In dimers with short spacers, polymers, carotenoid aggregates, and heteroacene crystals that demonstrate ^{1}(TT) emission, the nonradiative decay rate of ^{1}(TT) follows the gap-law dependence of their materials class (polyene or fused aromatic). This is to say that there is nothing surprising about the fast nonradiative decay exhibited by many singlet fission systems: It is a natural consequence of the fact that ^{1}(TT) is a pure spin singlet state. In other words, in the most strongly bound ^{1}(TT) states, ^{1}(TT) ceases to behave as a multiexciton. Instead, ^{1}(TT) behaves similarly to 2Ag in polyenes.

Materials with weakly interacting triplets [e.g., TIPS-tetracene (63) and well-spaced (91) or nonconjugated dimers (101)] show k_{nr} several orders of magnitude below that expected for a singlet state, as desired for singlet-fission photovoltaics. In these systems the orbital overlap is likely to be small, resulting in small J and negligible ΔE_{SQ}. These are likely to show mixed-spin triplet-pair states. It is interesting that even in these systems, ^{1}(TT) nonradiative decay is still closer to that of a singlet, rather than a triplet, suggesting that the triplets in ^{1}(TT) are nevertheless weakly

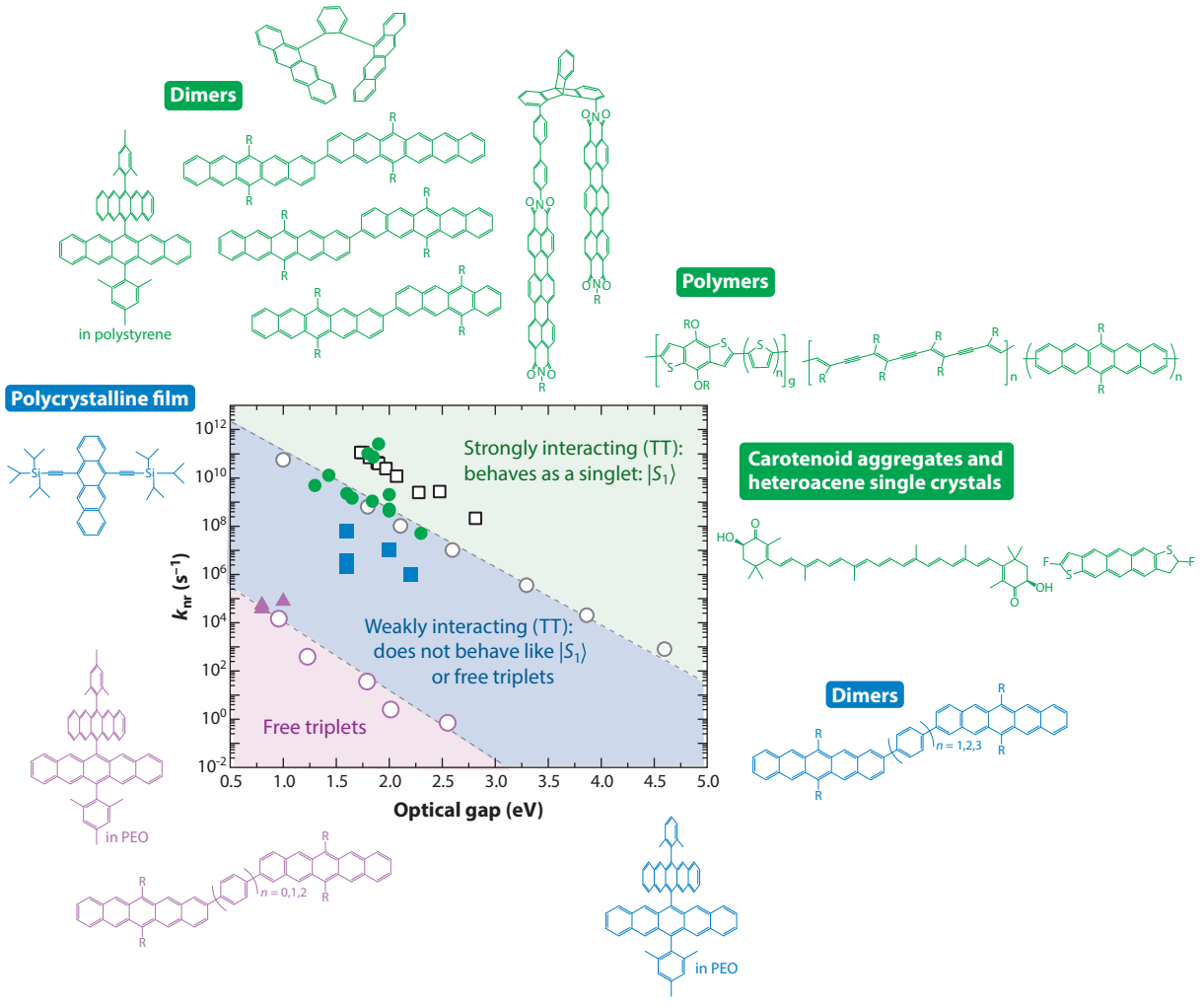

Figure 6

Gap law for nonradiative decay. The plot shows the nonradiative decay, k_{nr}, of 2Ag in carotenoids (*outlined black squares*) as a function of the 2Ag energy from Reference 137, of acenes from benzene to carbon nanotubes (*gray circles*) (110, 138), and of individual triplets in fused aromatic molecules (139, 140), as a function of $S_1^{(2)}$ and $T_1^{(2)}$ energy, respectively. The filled markers show the nonradiative decay and estimated electronic energy of ^{1}(TT) for the molecular structures shown around the figure (*color coded*). Abbreviation: PEO, poly(ethlylene oxide). Data extracted from References 36, 37, 53, 56, 58, 63, 65, 80, 83, 91, 94, 101, and 126.

interacting. Indeed, sensitization studies of the same pentacene dimers show that, while individual triplets follow the expected triplet gap law, singlet-fission-generated triplets decay significantly faster.

4. OBSERVATIONS OF WEAK OR MIXED SPIN STATES

It is likely that weakly coupled triplet pairs occur in almost all singlet-fission systems, for instance, as part of the TT separation pathway $^1(TT) \rightarrow (T\ldots T) \rightarrow T_1 + T_1$ (2, 30). However, direct optical detection of these states and distinction from noninteracting triplets are challenging. As discussed

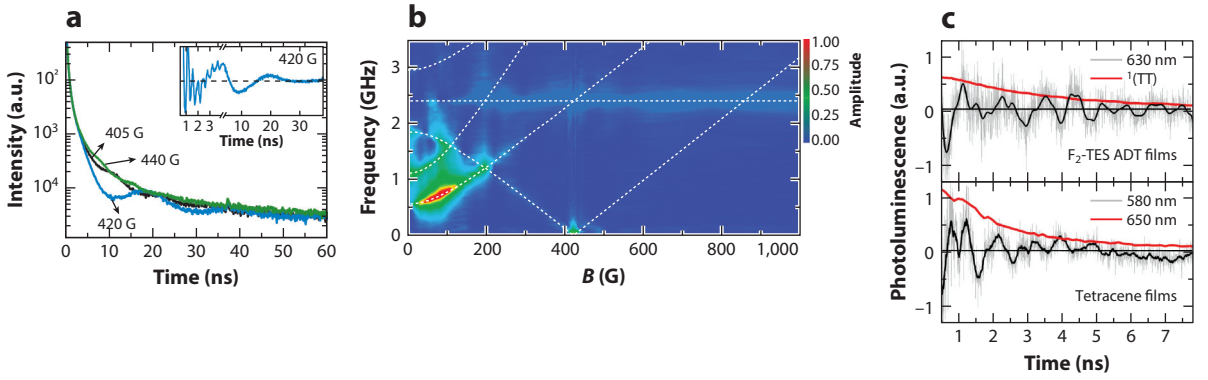

Figure 7

Photoluminescence quantum beating. (*a*) Beating is directly observed in photoluminescence decay kinetics, with field-dependent magnitude and frequency. (*Inset*) Subtraction of multi-exponential decay yields a pure beating signal. (*b*) Variation of beating magnitude and frequency as a function of field strength. The dashed lines show the expectation for noninteracting triplets. (*c*) The decay envelope of quantum beating kinetics in polycrystalline F_2-TES ADT and tetracene films [raw (*gray*) and smoothed (*black*)] closely tracks the population kinetics of a pure spin state ^{1}(TT) (*red*) measured separately. This is likely caused by dynamic equilibrium between pure and mixed-spin states. Panels *a* and *b* adapted from Reference 33, licensed under a Creative Commons Attribution 4.0 International License. Panel *c* adapted from Reference 65, licensed under a Creative Commons Attribution 4.0 International License.

above, these states are defined by negligible orbital overlap and configuration interaction, leading typically to an absence of ^{1}(TT)-specific excited-state absorption features.

The chief direct observable of weakly coupled triplet pairs in optical spectroscopy comes from photoluminescence quantum beating (33, 64, 65, 68, 69, 130). This phenomenon arises because ^{1}(TT) is not an energy eigenstate of the spin Hamiltonian under zero magnetic field in the absence of orbital overlap. Instead, it is a coherent superposition state $^1(\mathrm{TT}) = |S_1\rangle = \frac{1}{\sqrt{3}}(|xx\rangle + |yy\rangle + |zz\rangle)$. The component pair states, which each have mixed-spin character (25), acquire relative phases, leading to oscillations in the delayed fluorescence intensity with frequencies governed by the energy spacing between $|xx\rangle$, $|yy\rangle$, and $|zz\rangle$. At zero magnetic field, this phenomenon has now been observed in tetracene (68, 69, 130), F_2-TES ADT (65) and zethrenes (64), demonstrating that at least a small population of mixed-spin TT states is present in these materials.

To determine the energetic coupling between triplets within this weak-coupling regime, Wang et al. (33) measured quantum beating in tetracene under an applied magnetic field (**Figure 7*a*,*b***). The presence of an additional beat frequency at a field of 420 G was assigned to an anticrossing resonance due to the presence of triplet-triplet dipolar interaction (D_{AB} in Equation 6). Modeling their data gave $D_{AB} \sim 30$ neV, which, assuming the point-dipole approximation, suggests a triplet-pair separation of two to three times the lattice spacing.

A strikingly similar conclusion was reached through optically detected magnetic resonance measurements on TIPS-tetracene (21). This measurement, when using photoluminescence detection, is uniquely sensitive to weakly exchange-coupled triplet pairs, probing the regime where microwaves can drive a weakly emissive mixed ^{1}(TT)-^{5}(TT) state into pure, nonemissive ^{5}(TT) (21). Simulation of the data using a stochastic Liouville equation for the triplet-pair density matrix yielded a small triplet-triplet coupling, $D_{AB} \sim 60$ neV, corresponding to a separation of ~3 nm, or roughly two lattice spacings. It is also notable that these measurements observed such weakly coupled pairs on the same long timescales as the strongly exchange-coupled ^{5}(TT) signatures seen in EPR (Section 3.4.3).

5. WEAKLY AND STRONGLY COUPLED TRIPLET PAIRS IN THE SAME MATERIAL

Historically, singlet fission and triplet-triplet annihilation were described assuming weakly interacting triplet pairs with negligible orbital overlap. At the other extreme, triplet-pair states in polyenes were described as strongly coupled pure spin states, with significant orbital overlap (38, 39). It is now clear that both strongly coupled pure spin states $|S_1\rangle$ and weakly coupled mixed-spin states $|SQ\rangle$ can occur in the same material at the same time. The most studied materials where this is observed are tetracene and TIPS-tetracene films or crystals and isolated pentacene dimers. In tetracene, for example, the presence of ^{1}(TT) emission (65) and activated triplet-pair separation (67) suggests a population of strongly bound, pure spin states. At the same time, quantum beating (33, 68, 69) and an intertriplet dipolar coupling of only $D_{AB} \sim 30$ neV (33) suggest weakly bound, mixed-spin states. Interestingly, the fact that the quantum beating lifetime follows the ^{1}(TT) lifetime (**Figure 7*c***) suggests that both populations are in equilibrium at room temperature, a conclusion supported by recent emission measurements on TIPS-tetracene microcavities (131).

These observations can be reconciled through a dynamic equilibrium between weakly and strongly exchange-coupled triplet pairs. For example, the observation of strongly exchange-coupled ^{5}(TT) in EPR suggests that the system passes through $|S_1\rangle \rightarrow |SQ\rangle \rightarrow |S_1\rangle / |Q\rangle$ (36, 37) because singlet fission generates a singlet state, and in the presence of orbital overlap, without spin-orbit coupling, $|S_1\rangle$ cannot convert into $|Q\rangle$. A similar dynamic model was also proposed to explain high-magnetic-field measurements (23, 29). This model may provide an explanation for the very small magnitude of quantum beating observed in F_2-TES ADT or other materials (33, 64, 68, 69, 130), for instance, if the equilibrium favors pure $|S_1\rangle$.

Any process to account for this dynamic fluctuation must occur fast enough that spin coherence is not lost. A possible physical mechanism is low-frequency (intermolecular) vibrations: Calculations on organic thin films have shown that such off-diagonal dynamic disorder can give large (e.g., tens of milli–electron volts) fluctuations in short-range couplings such as the exchange interaction (132). Alternatively, the change in exchange coupling could be accomplished through triplet hopping. This idea is supported by the observation that weakly coupled $|SQ\rangle$ pairs in tetracene (33) and TIPS-tetracene (21) are separated by approximately two to three lattice spaces and that triplet hopping is estimated to occur on relatively fast, ~100-ps timescales, from modeling high-field effects (29, 133).

The salient point arising from these studies is that the couplings that govern TT interactions need not be fixed, even in molecular crystals, and care should be taken when interpreting experimental data in terms of a single parameter (e.g., exchange coupling).

6. CONCLUSIONS

Above we review recent literature in an attempt to develop a coherent picture of triplet-pair states in organic semiconductors. Our review suggests that in both intermolecular and intramolecular systems, singlet fission generates a pure spin, bound triplet-pair state ^{1}(TT) that is similar to the 2Ag state in carotenoids and other polyenes. In many systems, the ^{1}(TT) state appears to be in equilibrium with a population of weakly bound (mixed singlet/quintet) triplet-pair states so that pure singlet and quintet states exist in the same material at the same time as mixed singlet/quintet states. Having reviewed the literature, we find that several challenges and open questions remain.

The transition from ^{1}(TT) to (T…T) remains largely unexplored. This is partly because (T…T) is expected to have the same optical signatures as free triplets and the transition is therefore largely invisible (60). It is likely that transient EPR measurements (37), magnetic-field-dependent transient spectroscopy (134), or possibly quantum beating measurements (33) will uncover the

nature of these intermediate states: Do they remain coherent as they separate (2, 134, 135)? If so, how far can the individual triplets separate before they can no longer be described as (T…T)? It has been suggested that $|Q\rangle$ is a sequential step on the way to free triplets (102) [although this is not the most accepted model (31, 36, 37)]. Does $|Q\rangle$ have a distinct role in singlet fission, and if so, what is it? Beyond singlet fission, what is the role of these TT states in triplet-triplet annihilation and photon upconversion? Do the same stabilized intermediates form, and can they be utilized directly? Other avenues that remain to be explored are the definition of ^{1}(TT) binding energy in relation to the different experiments, the effect of morphology on ^{1}(TT) properties and its formation and decay dynamics, and the importance of static and dynamic disorder in describing triplet pairs.

We hope this review provides a snapshot of the current state of understanding of triplet-pair states in organic semiconductors and that in the coming years the rapid rate of research continues to provide answers to these questions.

DISCLOSURE STATEMENT

The authors are not aware of any affiliations, memberships, funding, or financial holdings that might be perceived as affecting the objectivity of this review.

ACKNOWLEDGMENTS

The authors would like to acknowledge the Engineering and Physical Sciences Research Council (EPSRC), grants EP/M025330/1, EP/N014022/1, and EP/S002103/1, as well as the University of Sheffield (Vice Chancellor's Fellowship scheme) for making this review possible.

LITERATURE CITED

1. Rao A, Friend RH. 2017. Harnessing singlet exciton fission to break the Shockley-Queisser limit. *Nat. Rev.* 2:17063
2. Scholes GD. 2015. Correlated pair states formed by singlet fission and exciton-exciton annihilation. *J. Phys. Chem. A* 119:12699–705
3. Casanova D. 2018. Theoretical modeling of singlet fission. *Chem. Rev.* 118:7164–207
4. Smith MB, Michl J. 2010. Singlet fission. *Chem. Rev.* 110:6891–936
5. Smith MB, Michl J. 2013. Recent advances in singlet fission. *Annu. Rev. Phys. Chem.* 64:361–86
6. Monahan NR, Sun D, Tamura H, Williams KW, Xu B, et al. 2017. Dynamics of the triplet pair state reveals the likely co-existence of coherent and incoherent singlet fission in crystalline hexacene. *Nat. Chem.* 9:341–46
7. Piland GB, Burdett JJ, Dillon RJ, Bardeen CJ. 2014. Singlet fission: from coherences to kinetics. *J. Phys. Chem. Lett.* 5:2312–19
8. Johnson JC, Nozik AJ, Michl J. 2013. The role of chromophore coupling in singlet fission. *Acc. Chem. Res.* 46:1290–99
9. Chan WL, Berkelbach TC, Provorse MR, Monahan NR, Tritsch JR, et al. 2013. The quantum coherent mechanism for singlet fission: experiment and theory. *Acc. Chem. Res.* 46:1321–29
10. Burdett JJ, Bardeen CJ. 2013. The dynamics of singlet fission in crystalline tetracene and covalent analogs. *Acc. Chem. Res.* 46:1312–20
11. Wilson MWB, Rao A, Ehrler B, Friend RH. 2013. Singlet exciton fission in polycrystalline pentacene: from photophysics toward devices. *Acc. Chem. Res.* 46:1330–38
12. Trinh MT, Pinkard A, Pun AB, Sanders SN, Kumarasamy E, et al. 2017. Distinct properties of the triplet pair state from singlet fission. *Sci. Adv.* 3:e1700241

13. Pensack RD, Tilley A, Grieco C, Purdum G, Ostroumov E, et al. 2018. Striking the right balance of intermolecular coupling for high-efficiency singlet fission. *Chem. Sci.* 9:6240–59
14. Burdett JJ, Piland GB, Bardeen CJ. 2013. Magnetic field effects and the role of spin states in singlet fission. *Chem. Phys. Lett.* 585:1–10
15. Spano FC, Silva C. 2014. H- and J-aggregate behavior in polymeric semiconductors. *Annu. Rev. Phys. Chem.* 65:477–500
16. Bardeen CJ. 2014. The structure and dynamics of molecular excitons. *Annu. Rev. Phys. Chem.* 65:127–48
17. Köhler A, Bässler H. 2009. Triplet states in organic semiconductors. *Mater. Sci. Eng. R* 66:71–109
18. Penfold TJ, Gindensperger E, Daniel C, Marian CM. 2018. Spin-vibronic mechanism for intersystem crossing. *Chem. Rev.* 118:6975–7025
19. Bencini A, Gatteschi D. 1990. The exchange interaction. In *EPR of Exchange Coupled Systems*, pp. 1–19. Berlin: Springer-Verlag
20. Richert S, Tait CE, Timmel CR. 2017. Delocalisation of photoexcited triplet states probed by transient EPR and hyperfine spectroscopy. *J. Magn. Reson.* 280:103–16
21. Bayliss SL, Chepelianskii AD, Sepe A, Walker BJ, Ehrler B, et al. 2014. Geminate and nongeminate recombination of triplet excitons formed by singlet fission. *Phys. Rev. Lett.* 112:238701
22. Kollmar C. 1993. Electronic structure of diradical and dicarbene intermediates in short-chain polydiacetylene oligomers. *J. Chem. Phys.* 98:7210–28
23. Yago T, Wakasa M. 2018. A spin exchange model for singlet fission. *Chem. Phys. Lett.* 695:240–44
24. Bardeen CJ. 2013. Excitonic processes in molecular crystalline materials. *MRS Bull.* 38:65–71
25. Merrifield RE. 1971. Magnetic effects on triplet exciton interactions. *Pure Appl. Chem.* 27:481–98
26. Kollmar C, Sixl H, Benk H, Denner V, Mahler G. 1982. Theory of two coupled triplet states—electrostatic energy splittings. *Chem. Phys. Lett.* 87:266–70
27. Bayliss SL, Weiss LR, Rao A, Friend RH, Chepelianskii AD, Greenham NC. 2016. Spin signatures of exchange-coupled triplet pairs formed by singlet fission. *Phys. Rev. B* 94:045204
28. Bayliss SL, Weiss LR, Mitioglu A, Galkowski K, Yang Z, et al. 2018. Site-selective measurement of coupled spin pairs in an organic semiconductor. *PNAS* 115:5077–82
29. Yago T, Ishikawa K, Katoh R, Wakasa M. 2016. Magnetic field effects on triplet pair generated by singlet fission in an organic crystal: application of radical pair model to triplet pair. *J. Phys. Chem. C* 120:27858–70
30. Wakasa M, Kaise M, Yago T, Katoh R, Wakikawa Y, Ikoma T. 2015. What can be learned from magnetic field effects on singlet fission: role of exchange interaction in excited triplet pairs. *J. Phys. Chem. C* 119:25840–44
31. Ishikawa K, Yago T, Wakasa M. 2018. Exploring the structure of an exchange-coupled triplet pair generated by singlet fission in crystalline diphenylhexatriene: anisotropic magnetic field effects on fluorescence in high fields. *J. Phys. Chem. C* 122:22264–72
32. Keevers TL, McCamey DR. 2016. Theory of triplet-triplet annihilation in optically detected magnetic resonance. *Phys. Rev. B* 93:045210
33. Wang R, Zhang C, Zhang B, Liu Y, Wang X, Xiao M. 2015. Magnetic dipolar interaction between correlated triplets created by singlet fission in tetracene crystals. *Nat. Commun.* 6:8602
34. Snaathorst D, Keijzers C. 1984. Triplet-triplet interactions between dimers of a copper maleonitriledithiolate complex. *Mol. Phys.* 51:509–24
35. Benk H, Sixl H. 1981. Theory of triplet-triplet annihilation in optically detected magnetic resonance. *Mol. Phys.* 42:779–801
36. Weiss LR, Bayliss SL, Kraffert F, Thorley KJ, Anthony JE, et al. 2016. Strongly exchange-coupled triplet pairs in an organic semiconductor. *Nat. Phys.* 13:176–81
37. Tayebjee MJY, Sanders SN, Kumarasamy E, Campos LM, Sfeir MY, McCamey DR. 2016. Quintet multiexciton dynamics in singlet fission. *Nat. Phys.* 13:182–88
38. Barford W, Bursill JR, Yu LM. 2001. Density-matrix renormalization-group calculations of excited states of linear polyenes. *Phys. Rev. B* 65:195108

39. Hu W, Chan GKL. 2015. Excited-state geometry optimization with the density matrix renormalization group, as applied to polyenes. *J. Chem. Theory Comput.* 11:3000–9
40. Feng X, Krylov AI. 2016. On couplings and excimers: lessons from studies of singlet fission in covalently linked tetracene dimers. *Phys. Chem. Chem. Phys.* 18:7751–61
41. Suna A. 1970. Kinematics of exciton-exciton annihilation in molecular crystals. *Phys. Rev. B* 1:1716–39
42. Tavan P, Schulten K. 1987. Electronic excitations in finite and infinite polyenes. *Phys. Rev. B* 36:4337–58
43. Barford W. 2005. *Electronic and Optical Properties of Conjugated Polymers*. New York: Oxford Univ. Press. 1st ed.
44. Josue JS, Frank HA. 2002. Direct determination of the S_1 excited-state energies of xanthophylls by low-temperature fluorescence spectroscopy. *J. Phys. Chem. A* 106:4815–24
45. Petek H, Bell AJ, Choi YS, Yoshihara K, Tounge BA, Christensen RL. 1993. The 2^1A_g state of *trans*, *trans*-1,3,5,7-octatetraene in free jet expansions. *J. Chem. Phys.* 98:3777–94
46. Merrifield RE. 1968. Diffusion and mutual annihilation of triplet excitons in organic crystals. *Acc. Chem. Res.* 1:129–35
47. Zimmerman PM, Zhang Z, Musgrave CB. 2010. Singlet fission in pentacene through multi-exciton quantum states. *Nat. Chem.* 2:648–52
48. Chan WL, Ligges M, Jailaubekov A, Kaake L, Miaja-Avila L, Zhu XY. 2011. Observing the multiexciton state in singlet fission and ensuing ultrafast multielectron transfer. *Science* 334:1541–45
49. Zeng T, Ananth N, Hoffmann R. 2014. Seeking small molecules for singlet fission: a heteroatom substitution strategy. *J. Am. Chem. Soc.* 136:12638–47
50. Yost SR, Lee J, Wilson MWB, Wu T, McMahon DP, et al. 2014. A transferable model for singlet-fission kinetics. *Nat. Chem.* 6:492–97
51. Burdett JJ, Gosztola D, Bardeen CJ. 2011. The dependence of singlet exciton relaxation on excitation density and temperature in polycrystalline tetracene thin films: kinetic evidence for a dark intermediate state and implications for singlet fission. *J. Chem. Phys.* 135:214508
52. Tayebjee MJY, Clady RGCR, Schmidts TW. 2013. The exciton dynamics in tetracene thin films. *Phys. Chem. Chem. Phys.* 15:14797–805
53. Stern HL, Musser AJ, Gelinas S, Parkinson P, Herz LM, et al. 2015. Identification of a triplet pair intermediate in singlet exciton fission in solution. *PNAS* 112:7656–61
54. Walker BJ, Musser AJ, Beljonne D, Friend RH. 2013. Singlet exciton fission in solution. *Nat. Chem.* 5:1019–24
55. Dover CB, Gallaher JK, Frazer L, Tapping PC, Petty AJ II, et al. 2018. Endothermic singlet fission is hindered by excimer formation. *Nat. Chem.* 10:305–10
56. Musser AJ, Liebel M, Schnedermann C, Wende T, Kehoe TB, et al. 2015. Evidence for conical intersection dynamics mediating ultrafast singlet exciton fission. *Nat. Phys.* 11:352–57
57. Bakulin AA, Morgan SE, Kehoe TB, Wilson MWB, Chin AW, et al. 2016. Real-time observation of multiexcitonic states in ultrafast singlet fission using coherent 2D electronic spectroscopy. *Nat. Chem.* 8:16–23
58. Korovina NV, Das S, Nett Z, Feng X, Joy J, et al. 2016. Singlet fission in a covalently linked cofacial alkynyltetracene dimer. *J. Am. Chem. Soc.* 138:617–27
59. Pensack RD, Tilley AJ, Parkin SR, Lee TS, Payne MM, et al. 2015. Exciton delocalization drives rapid singlet fission in nanoparticles of acene derivatives. *J. Am. Chem. Soc.* 137:6790–803
60. Pensack RD, Ostroumov EE, Tilley AJ, Mazza S, Grieco C, et al. 2016. Observation of two triplet-pair intermediates in singlet exciton fission. *J. Phys. Chem. Lett.* 7:2370–75
61. Herz J, Buckup T, Paulus F, Engelhart JU, Bunz UHF, Motzkus M. 2015. Unveiling singlet fission mediating states in TIPS-pentacene and its aza derivatives. *J. Phys. Chem. A* 119:6602–10
62. Mauck CM, Hartnett PE, Margulies EA, Ma L, Miller CE, et al. 2016. Singlet fission via an excimer-like intermediate in 3,6-bis(thiophen-2-yl)diketopyrrolopyrrole derivatives. *J. Am. Chem. Soc.* 138:11749–61
63. Stern HL, Cheminal A, Yost SR, Broch K, Bayliss SL, et al. 2017. Vibronically coherent ultrafast triplet-pair formation and subsequent thermally activated dissociation control efficient endothermic singlet fission. *Nat. Chem.* 9:1205–12

64. Lukman S, Richter JM, Yang L, Hu P, Wu J, et al. 2017. Efficient singlet fission and triplet-pair emission in a family of zethrene diradicaloids. *J. Am. Chem. Soc.* 139:18376–85
65. Yong CK, Musser AJ, Bayliss SL, Lukman S, Tamura H, et al. 2017. The entangled triplet pair state in acene and heteroacene materials. *Nat. Commun.* 8:15953
66. Aoki-Matsumoto T, Furuta K, Yamada T, Moriya H, Mizuno K. 2001. Exciton photoluminescence in pentacene single crystal. *Int. J. Mod. Phys. B* 15:3753–56
67. Wilson MW, Rao A, Johnson K, Gelinas S, Di Pietro R, et al. 2013. Temperature-independent singlet exciton fission in tetracene. *J. Am. Chem. Soc.* 135:16680–88
68. Chabr M, Wild UP, Fünfschilling J, Zschokke-Gränacher I. 1981. Quantum beats of prompt fluorescence in tetracene crystals. *Chem. Phys.* 57:425–30
69. Burdett JJ, Bardeen CJ. 2012. Quantum beats in crystalline tetracene delayed fluorescence due to triplet pair coherences produced by direct singlet fission. *J. Am. Chem. Soc.* 134:8597–607
70. Müller HP, Thoma P, Vaubel G. 1967. The phosphorescence of anthracene single crystals and its spectrum. *Phys. Status Solidi* 23:253–62
71. Anger F, Oss JO, Heinemeyer U, Broch K, Scholz R, et al. 2012. Photoluminescence spectroscopy of pure pentacene, perfluoropentacene, and mixed thin films. *J. Chem. Phys.* 136:054701
72. Lim SH, Bjorklund TG, Spano FC, Bardeen CJ. 2004. Exciton delocalization and superradiance in tetracene thin films and nanoaggregates. *Phys. Rev. Lett.* 92:107402
73. Sprafke JK, Kondratuk DV, Wykes M, Thompson AL, Ho M, et al. 2011. Belt-shaped π-systems: relating geometry to electronic structure in a six-porphyrin nanoring. *J. Am. Chem. Soc.* 133:17262–73
74. Greco JA, LaFountain AM, Kinashi N, Shinada T, Sakaguchi K, et al. 2016. Spectroscopic investigation of the carotenoid deoxyperidinin: direct observation of the forbidden $S_0 \rightarrow S_1$ transition. *J. Phys. Chem. B* 120:2731–44
75. Niedzwiedzki DM, Blankenship RE. 2018. Excited-state properties of the central-*cis* isomer of the carotenoid peridinin. *Arch. Biochem. Biophys.* 649:29–36
76. Josue JS, Frank HA. 2002. Direct determination of the S_1 excited-state energies of xanthophylls by low-temperature fluorescence spectroscopy. *J. Phys. Chem. A* 106:4815–24
77. Polívka T, Sundström V. 2004. Ultrafast dynamics of carotenoid excited states—from solution to natural and artificial systems. *Chem. Rev.* 104:2021–71
78. Herkstroeter WG. 1975. Triplet energies of azulene, beta-carotene and ferrocene. *J. Am. Phys. Soc.* 97:4161–67
79. Piland GB, Bardeen CJ. 2015. How morphology affects singlet fission in crystalline tetracene. *J. Phys. Chem. Lett.* 6:1841–46
80. Busby E, Xia J, Wu Q, Low JZ, Song R, et al. 2015. A design strategy for intramolecular singlet fission mediated by charge-transfer states in donor-acceptor organic materials. *Nat. Mater.* 14:426–33
81. Hu J, Xu K, Shen L, Wu Q, He G, et al. 2018. New insights into the design of conjugated polymers for intramolecular singlet fission. *Nat. Commun.* 9:2999
82. Aryanpour K, Shukla A, Mazumdar S. 2015. Theory of singlet fission in polyenes, acene crystals, and covalently linked acene dimers. *J. Phys. Chem. C* 119:6966–79
83. Margulies EA, Logsdon JL, Miller CE, Ma L, Simonoff E, et al. 2017. Direct observation of a charge-transfer state preceding high-yield singlet fission in terrylenediimide thin films. *J. Am. Chem. Soc.* 139:663–71
84. Breen I, Tempelaar R, Bizimana LA, Kloss B, Reichman DR, Turner DB. 2017. Triplet separation drives singlet fission after femtosecond correlated triplet pair production in rubrene. *J. Am. Chem. Soc.* 139:11745–51
85. Grieco C, Kennehan ER, Rimshaw A, Payne MM, Anthony JE, Asbury JB. 2017. Harnessing molecular vibrations to probe triplet dynamics during singlet fission. *J. Phys. Chem. Lett.* 8:5700–6
86. Folie BD, Haber JB, Refaely-Abramson S, Neaton JB, Ginsberg NS. 2018. Long-lived correlated triplet pairs in a π-stacked crystalline pentacene derivative. *J. Am. Chem. Soc.* 140:2326–35
87. Feng X, Luzanov AV, Krylov AI. 2013. Fission of entangled spins: an electronic structure perspective. *J. Phys. Chem. Lett.* 4:3845–52

88. Chien AD, Zimmerman PM. 2017. Recovering dynamic correlation in spin flip configuration interaction through a difference dedicated approach. *J. Chem. Phys.* 146:014103
89. Khan S, Mazumdar S. 2017. Diagrammatic exciton basis theory of the photophysics of pentacene dimers. *J. Phys. Chem. Lett.* 8:4468–78
90. Khan S, Mazumdar S. 2017. Theory of transient excited state absorptions in pentacene and derivatives: triplet-triplet biexciton versus free triplets. *J. Phys. Chem. Lett.* 8:5943–48
91. Sanders SN, Kumarasamy E, Pun AB, Trinh MT, Choi B, et al. 2015. Quantitative intramolecular singlet fission in bipentacenes. *J. Am. Chem. Soc.* 137:8965–72
92. Wilson MWB, Rao A, Clark J, Kumar RSS, Brida D, et al. 2011. Ultrafast dynamics of exciton fission in polycrystalline pentacene. *J. Am. Chem. Soc.* 133:11830–33
93. Rao A, Wilson MWB, Hodgkiss JM, Albert-Seifried S, Bässler H, Friend RH. 2010. Exciton fission and charge generation via triplet excitons in pentacene/C_{60} bilayers. *J. Am. Chem. Soc.* 132:12698–703
94. Sanders SN, Kumarasamy E, Pun AB, Steigerwald ML, Sfeir MY, Campos LM. 2016. Intramolecular singlet fission in oligoacene heterodimers. *Angew. Chem. Int. Ed.* 55:3373–77
95. Sanders SN, Kumarasamy E, Pun AB, Steigerwald ML, Sfeir MY, Campos LM. 2016. Singlet fission in polypentacene. *Chemistry* 1:505–11
96. Zirzlmeier J, Lehnherr D, Coto PB, Chernick ET, Casillas R, et al. 2015. Singlet fission in pentacene dimers. *PNAS* 112:5325–30
97. Wang X, Wang R, Shen L, Tang Z, Wen CY, et al. 2018. Intramolecular singlet fission in a face-to-face stacked tetracene trimer. *Phys. Chem. Chem. Phys.* 20:6330–36
98. Sakuma T, Sakai H, Araki Y, Mori T, Wada T, et al. 2016. Long-lived triplet excited states of bent-shaped pentacene dimers by intramolecular singlet fission. *J. Phys. Chem. A* 120:1867–75
99. Yamakado T, Takahashi S, Watanabe K, Matsumoto Y, Osuka A, Saito S. 2018. Conformational planarization versus singlet fission: distinct excited-state dynamics of cyclooctatetraene-fused acene dimers. *Angew. Chem. Int. Ed.* 57:5438–43
100. Lukman S, Musser AJ, Chen K, Athanasopoulos S, Yong CK, et al. 2015. Tuneable singlet exciton fission and triplet-triplet annihilation in an orthogonal pentacene dimer. *Adv. Funct. Mater.* 25:5452–61
101. Lukman S, Chen K, Hodgkiss JM, Turban DH, Hine ND, et al. 2016. Tuning the role of charge-transfer states in intramolecular singlet exciton fission through side-group engineering. *Nat. Commun.* 7:13622
102. Basel BS, Zirzlmeier J, Hetzer C, Phelan BT, Krzyaniak MD, et al. 2017. Unified model for singlet fission within a non-conjugated covalent pentacene dimer. *Nat. Commun.* 8:15171
103. Kumarasamy E, Sanders SN, Tayebjee MJY, Asadpoordarvish A, Hele TJH, et al. 2017. Tuning singlet fission in π-bridge-π chromophores. *J. Am. Chem. Soc.* 139:12488–94
104. Polak D, Musser AJ, Sutherland GA, Auty A, Branchi F, et al. 2019. Band-edge excitation of carotenoids removes S* revealing triplet-pair contributions to the S1 absorption spectrum. arXiv:1901.04900 [physics.chem-ph]
105. Dillon RJ, Piland GB, Bardeen CJ. 2013. Different rates of singlet fission in monoclinic versus orthorhombic crystal forms of diphenylhexatriene. *J. Am. Chem. Soc.* 135:17278–81
106. Cheveigne S, Klejn J, Leger A, Belin M, Defourneau D. 1977. Molecular electronic transitions observed by inelastic tunneling spectroscopy. *Phys. Rev. B* 15:750–54
107. Nijegorodov N, Ramachandran V, Winkoun DP. 1997. The dependence of the absorption and fluorescence parameters, the intersystem crossing and internal conversion rate constants on the number of rings in polyacene molecules. *Spectrochim. Acta A* 53:1813–24
108. Mcglynn SP, Padhye MR, Kasha M. 1955. Lowest triplet levels of the polyacenes. *J. Chem. Phys.* 23:593–94
109. Reineke S, Baldo MA. 2013. Room temperature triplet state spectroscopy of organic semiconductors. *Sci. Rep.* 4:3797
110. Nijegorodov N, Ramachandran V, Winkoun D. 1997. The dependence of the absorption and fluorescence parameters, the intersystem crossing and internal conversion rate constants on the number of rings in polyacene molecules. *Spectrochim. Acta A* 53:1813–24

111. Vilar MR, Heyman M, Schott M. 1983. Spectroscopy of low-energy electrons backscattered from an organic solid surface: pentacene. *Chem. Phys. Lett.* 94:522–26
112. Burgos J, Pope M, Swenberg CE, Alfano RR. 1977. Heterofission in pentacene doped tetracene single crystals. *Phys. Status Solidi B* 83:249–56
113. Tomkiewicz Y, Groff RP, Avakian P. 1971. Spectroscopic approach to energetics of exciton fission and fusion in tetracene crystals. *J. Chem. Phys.* 54:4504–7
114. Yarmus L, Rosenthal J, Chopp M. 1972. EPR of triplet excitions in tetracene crystals: spin polarization and the role of singlet exciton fission. *Chem. Phys. Lett.* 16:477–81
115. Klenina IB, Makhneva ZK, Moskalenko AA, Kuzmin AN, Proskuryakov II. 2013. Singlet-triplet excitation fission in light-harvesting complexes of photosynthetic bacteria and in isolated carotenoids. *Biophysics* 58:43–50
116. Klenina IB, Makhneva ZK, Moskalenko AA, Gudkov ND, Bolshakov MA, et al. 2014. Singlet-triplet fission of carotenoid excitation in light-harvesting LH2 complexes of purple phototrophic bacteria. *Biochemistry (Moscow)* 79:235–41
117. Lubert-Perquel D, Salvadori E, Dyson M, Stavrinou PN, Montis R, et al. 2018. Identifying triplet pathways in dilute pentacene films. *Nat. Commun.* 9:4222
118. Pensack RD, Grieco C, Purdum GE, Mazza SM, Tilley AJ, et al. 2017. Solution-processable, crystalline material for quantitative singlet fission. *Mater. Horiz.* 4:915–23
119. Grieco C, Doucette GS, Munro JM, Kennehan ER, Lee Y, et al. 2017. Triplet transfer mediates triplet pair separation during singlet fission in 6,13-bis(triisopropylsilylethynyl)-pentacene. *Adv. Funct. Mater.* 27:1703929
120. Grieco C, Kennehan ER, Kim H, Pensack RD, Brigeman AN, et al. 2018. Direct observation of correlated triplet pair dynamics during singlet fission using ultrafast mid-IR spectroscopy. *J. Phys. Chem. C* 122:2012–22
121. Pun AB, Sanders SN, Kumarasamy E, Sfeir MY, Congreve DN, Campos LM. 2017. Triplet harvesting from intramolecular singlet fission in polytetracene. *Adv. Mater.* 29:1701416
122. Lee TS, Lin YL, Kim H, Pensack RD, Rand BP, Scholes GD. 2018. Triplet energy transfer governs the dissociation of the correlated triplet pair in exothermic singlet fission. *J. Phys. Chem. Lett.* 9:4087–95
123. Pace NA, Arias DH, Granger DB, Christensen S, Anthony JE, Johnson JC. 2018. Dynamics of singlet fission and electron injection in self-assembled acene monolayers on titanium dioxide. *Chem. Sci.* 9:3004–13
124. Le AK, Bender JA, Arias DH, Cotton DE, Johnson JC, Roberts ST. 2018. Singlet fission involves an interplay between energetic driving force and electronic coupling in perylenediimide films. *J. Am. Chem. Soc.* 140:814–26
125. Chan WL, Ligges M, Zhu XY. 2012. The energy barrier in singlet fission can be overcome through coherent coupling and entropic gain. *Nat. Chem.* 4:840–45
126. Lanzani G, Stagira S, Cerullo G, De Silvestri S, Comoretto D, et al. 1999. Triplet exciton generation and decay in a red polydiacetylene studied by femtosecond spectroscopy. *Chem. Phys. Lett.* 313:525–32
127. Musser AJ, Al-Hashimi M, Maiuri M, Brida D, Heeney M, et al. 2013. Activated singlet exciton fission in a semiconducting polymer. *J. Am. Chem. Soc.* 135:12747–54
128. Lanzani G, Cerullo G, Zavelani-Rossi M, De Silvestri S, Comoretto D, et al. 2001. Triplet-exciton generation mechanism in a new soluble (red-phase) polydiacetylene. *Phys. Rev. Lett.* 87:187402
129. Musser AJ, Maiuri M, Brida D, Cerullo G, Friend RH, Clark J. 2015. The nature of singlet exciton fission in carotenoid aggregates. *J. Am. Chem. Soc.* 137:5130–39
130. Fünfschilling J. 1985. Quantum beats in the fluorescence decay of tetracene crystals. *J. Phys. Colloq.* 46:377–80
131. Polak D, Jayaprakash R, Leventis A, Fallon KJ, Coulthard H, et al. 2018. Manipulating matter with strong coupling: harvesting triplet excitons in organic exciton microcavities. arXiv:1806.09990 [cond-mat.mtrl-sci]
132. Aragó J, Troisi A. 2015. Dynamics of the excitonic coupling in organic crystals. *Phys. Rev. Lett.* 114:026402
133. Wakasa M, Yago T, Sonoda Y, Katoh R. 2018. Structure and dynamics of triplet-exciton pairs generated from singlet fission studied via magnetic field effects. *Commun. Chem.* 1:9

134. Huynh UNV, Basel TP, Ehrenfreund E, Li G, Yang Y, et al. 2017. Transient magnetophotoinduced absorption studies of photoexcitations in π-conjugated donor-acceptor copolymers. *Phys. Rev. Lett.* 119:017401
135. Teichen PE, Eaves JD. 2015. Collective aspects of singlet fission in molecular crystals. *J. Chem. Phys.* 143:044118
136. Yamagata H, Norton J, Hontz E, Olivier Y, Beljonne D, et al. 2011. The nature of singlet excitons in oligoacene molecular crystals. *J. Chem. Phys.* 134:204703
137. Chynwat V, Frank HA. 1995. The application of the energy gap law to the S_1 energies and dynamics of carotenoids. *Chem. Phys.* 194:237–44
138. Wang F, Dukovic G, Brus LE, Heinz TF. 2004. Time-resolved fluorescence of carbon nanotubes and its implication for radiative lifetimes. *Phys. Rev. Lett.* 92:177401
139. Clarke RH, Frank HA. 1976. Triplet state radiationless transitions in polycyclic hydrocarbons. *J. Chem. Phys.* 65:39–47
140. Yu HL, Lin TS, Weissman SI, Sloop DJ. 1984. Time resolved studies of pentacene triplets by electron spin echo spectroscopy. *J. Chem. Phys.* 80:102–7

Annual Review of
Physical Chemistry
Volume 70, 2019

Contents

Errata

An online log of corrections to *Annual Review of Physical Chemistry* articles may be found at http://www.annualreviews.org/errata/physchem